frontiers | Frontiers in Batteries and Electrochemistry

TYPE Review
PUBLISHED 05 February 2024
DOI 10.3389/fbael.2024.1353886

OPEN ACCESS

EDITED BY
Jacob Joseph Lamb,
Norwegian University of Science and Technology, Norway

REVIEWED BY
Jin Cao,
China Three Gorges University, China
Zachary G. Neale,
Naval Research Laboratory, United States

*CORRESPONDENCE
Vaiyapuri Soundharrajan,
Soundharrajan.Vaiyapuri@uni-muenster.de
Duong Pham Tung,
duong.mse.hust@gmail.com
Jung Ho Kim,
jhk@uow.edu.au
Jaekook Kim,
jaekook@chonnam.ac.kr

†These authors have contributed equally to this work

RECEIVED 11 December 2023
ACCEPTED 15 January 2024
PUBLISHED 05 February 2024

CITATION
Soundharrajan V, Nithiananth S, Muthukrishnan AP, Singh G, Arifiadi A, Tung DP, Kim JH and Kim J (2024), Mn deposition/dissolution chemistry and its contemporary application in R&D of aqueous batteries. *Front. Batteries Electrochem.* 3:1353886. doi: 10.3389/fbael.2024.1353886

Mn deposition/dissolution chemistry and its contemporary application in R&D of aqueous batteries

Vaiyapuri Soundharrajan[1*†], Subramanian Nithiananth[2†], Akshaiya Padmalatha Muthukrishnan[3], Gita Singh[4], Anindityo Arifiadi[1,5], Duong Pham Tung[6*], Jung Ho Kim[7*] and Jaekook Kim[8*]

[1]MEET Battery Research Center, Institute of Physical Chemistry, Westfalische Wilhelms-Universitat Munster, Münster, Germany, [2]Graduate School of Science and Technology, Shizuoka University, Hamamatsu, Shizuoka, Japan, [3]School of Energy Engineering, Kyungpook National University, Daegu, Republic of Korea, [4]School of Chemistry, University College Dublin, Belfield, Ireland, [5]International Graduate School for Battery Chemistry Characterization, Analysis Recycling and Application (BACCARA), University of Münster, Münster, Germany, [6]School of Engineering Physics, Hanoi University of Science and Technology, Hanoi, Vietnam, [7]Institute for Superconducting and Electronic Materials (ISEM), Australian Institute of Innovative Materials (AIIM), University of Wollongong, North Wollongong, NSW, Australia, [8]Research Center for Artificial Intelligence Assisted Ionics Based Materials Development Platform, Chonnam National University, Gwangju, Republic of Korea

The advancement of Mn deposition/dissolution chemistry and its translation to different battery variants is progressively documented. However, Mn represents poor reversibility, causing limitations for practical application. With the purpose of improving Mn-based battery operation, various technical solutions have been implemented for numerous batteries with Mn deposition/dissolution chemistry. This review summarizes the rapid advancements on Mn deposition/dissolution chemistry-based aqueous batteries.

KEYWORDS

Mn deposition/dissolution chemistry, ARBs, metal anodes, electrolyte additive, gas evolution

1 Introduction

The development of a safe, clean, and affordable energy storage device to tackle the environmental impact of fossil fuels has been a major objective for researchers globally (Larcher and Tarascon, 2015; Ming et al., 2019; Soundharrajan et al., 2022b). Li-ion batteries (LIBs) are well-known as the current gold standard for energy storage, especially in long-range electric vehicles (EVs), owing to their high energy and power density. (Scarfogliero et al., 2018; Chen et al., 2020; Soundharrajan et al., 2022c). To reduce the carbon footprint of EV charging, electricity generation from renewable energy sources, such as solar and wind, must be increased, and grid-scale energy-storage is required to handle the intermittent nature of renewable energy (Zhu et al., 2022). For this application, the use of low-cost and low-energy aqueous rechargeable batteries (ARBs), in which the size of the battery is not an issue, is often considered to be a compelling choice (Zeng et al., 2019; Soundharrajan et al., 2023).

ARBs with Mn deposition/dissolution reaction mechanisms have caught the eyes of energy researchers and are expected as one of the most promising energy storage host for

stationary and home electronic devices. The aim of this review article is to summarise the classical evolution of Mn deposition/dissolution chemistry and debates on the resolution of the mechanism in different cathode/anode and electrolyte combinations. A general introduction to aqueous batteries and how they've evolved over the years is given. Then, we discuss the origin of Mn deposition and dissolution chemistry and its potential application in electrochemical energy storage devices. Further, we discuss the actual possibilities of Mn-deposition and dissolution chemistry for the capacity performance of Mn-supported cathodes for zinc-ion batteries (ZIB). Finally, the adaptation of the Mn deposition/dissolution chemistry for the formulation of different ARBs with different metal anodes and their reaction mechanism is discussed.

2 Overview of the evolutions of aqueous rechargeable batteries

ARBs have been dominating the energy-storage market for more than a century after the invention of the rechargeable Pb-acid battery by Wilhelm Sinsteden and later by Gaston Plante (Kurzweil, 2010). After 170 years, the Pb-acid battery continues to be an important energy-storage device used in day-to-day applications, such as starting batteries for cars and grid storage (Shin and Choi, 2020). After the original invention of Pb-acid batteries, many rechargeable battery technologies emerged, such as the Ni||Cd, Metal||Hydride, and Ni||Zn batteries. While the discovery of MnO_2||Zn primary battery by Georges-Lionel Leclanché has been translated into commercial portable electronic devices (Lim et al., 2021; Durena and Zukuls, 2023; Feng et al., 2023).

Highly alkaline KOH electrolytes with high pH values in the range of 9–14 was initially used in the above Durena mentioned Zn-Mn batteries, and their cycle life were typically limited to <50 cycles (Kordesch et al., 1981). This urged scientists to identify an electrolyte replacement, and accordingly, in 1986, Yamamoto and Shoji (Yamamoto and Shoji, 1986) swapped the traditional alkaline electrolyte with a mildly aqueous $ZnSO_4$ electrolyte. This concept was later developed as a ZIB in 2011 based on the Zn^{2+} shuttling properties, and this battery is considerably different from the conversion-based alkaline Zn-Mn batteries (Xu et al., 2012). Subsequently, in 1994, Wu et al. (Li et al., 1994) demonstrated aqueous rechargeable Li-ion batteries using a $LiMn_2O_4$ cathode and a VO_2 anode. The battery operates based on Li^+ shuttling between the anode and cathode, similar to that in non-aqueous LIBs. Since the discovery of the intercalation chemistry of aqueous systems, substantial advancements have resulted in several rocking-chair-type aqueous batteries, including monovalent and multivalent metal-ion batteries (Liu et al., 2018). Recently, hybrid batteries consisting of an intercalation-type cathode paired with a metal anode or intercalation anode paired with metal oxides/sulfides were documented (Soundharrajan et al., 2018; Ao et al., 2019). The recently reported new Mn-H battery driven by the Mn oxidation reaction/Mn reduction reaction (MOR/MRR), i.e., Mn deposition/dissolution chemistry, generated the potential for new energy storage devices (Chen et al., 2018). This review provides a brief overview of the development of Mn-based batteries, starting from the discovery of rechargeable MnO_2||Zn batteries, followed by the efforts to understand the insertion conversion and deposition/dissolution reaction mechanisms in Mn-based aqueous batteries. Finally, we highlight the diverse cell setups employing Mn dissolution/deposition chemistry and the strategy to enable the stable cycling of these batteries.

3 Mn deposition/dissolution chemistry: a potential concept for the energy-storage sector?

Before reviewing the MnO_2/Mn^{2+}-chemistry-inspired energy storage devices in detail, the mechanistical or historical aspects of MOR/MRR must be understood (Soundharrajan et al., 2022a). Although several reports regarding modern-day battery devices inspired by MnO_2/Mn^{2+} chemistry have been published recently (Moon et al., 2021; Zheng et al., 2021; Liu et al., 2022a; Yang et al., 2022; Naresh et al., 2023; Ye et al., 2023), the observation of unique MnO_2/Mn^{2+} chemistry was first reported in 1998 in relation to the $Zn/ZnSO_4/MnO_2$ rechargeable cell by Kim et al. (Kim and Oh, 1998). Although the $Zn/ZnSO_4/MnO_2$ rechargeable cell was not coined as ZIBs by Kim et al. (Kim and Oh, 1998), the use of mild-aqueous $ZnSO_4$ electrolyte for Zn/MnO_2 rechargeable cells could termed as ZIBs, as per the recent nomenclature. More specifically, the authors observed the dissolution of solid-MnO_2 cathode into soluble Mn^{2+} ions during the discharge process, whereas the soluble Mn^{2+} ions were re-deposited to form solid-MnO_2 during the charging process. More importantly, the authors found that dissolved Mn^{2+} ions were not completely re-deposited during the repeated charge/discharge cycles in the $ZnSO_4$ electrolyte. The authors attributed this inefficiency to the nature of the conductive-carbon surface states used for electrode fabrication. To validate their claim, the authors compared the MnO_2/Mn^{2+} chemistry of different carbon sources belonging to the acetylene and furnace black categories using cyclic voltammetry (CV). Based on the comparative CV and *ex-situ* scanning electron microscope (SEM) outputs, they confirmed that the cathode loaded with acetylene black with negligible surface oxygen species exhibited better MnO_2/Mn^{2+} reversibility than the other carbon sources because the lack of surface oxygen species increased facile Mn^{2+} oxidation. Additionally, they demonstrated that the reversibility of MnO_2/Mn^{2+} redox can be improved through the addition of $MnSO_4$ to the $ZnSO_4$ electrolyte. Here, the presence of $MnSO_4$ can suppress non-faradaic Mn dissolution and the formation of $ZnSO_4$ deposits on the cathode surface.

Kim et al. (Kim and Oh, 1998) initially investigated the electrolyte-induced MnO_2/Mn^{2+} chemistry on a solid-state cathode used in a Zn/MnO_2 rechargeable cell. Perret et al. (Perret et al., 2011) harvested the charge supplied by the *in situ* reversible MnO_2/Mn^{2+} chemistry by employing electrolytic Mn as the main means of charge storage almost a decade later in 2011. More specifically, the authors constructed a hybrid supercapacitor with composite graphene as a capacitive electrode and graphene as the battery-type electrode that acted as a substrate for the *in situ* electrochemical deposition/dissolution of MnO_2 in 0.5 M H_2SO_4 + 0.5 M $MnSO_4$ electrolyte. They observed that the dissolution/deposition efficiency of MnO_2 was only 80%, which indicates that only ~80% of the deposited MnO_2 dissolved into the

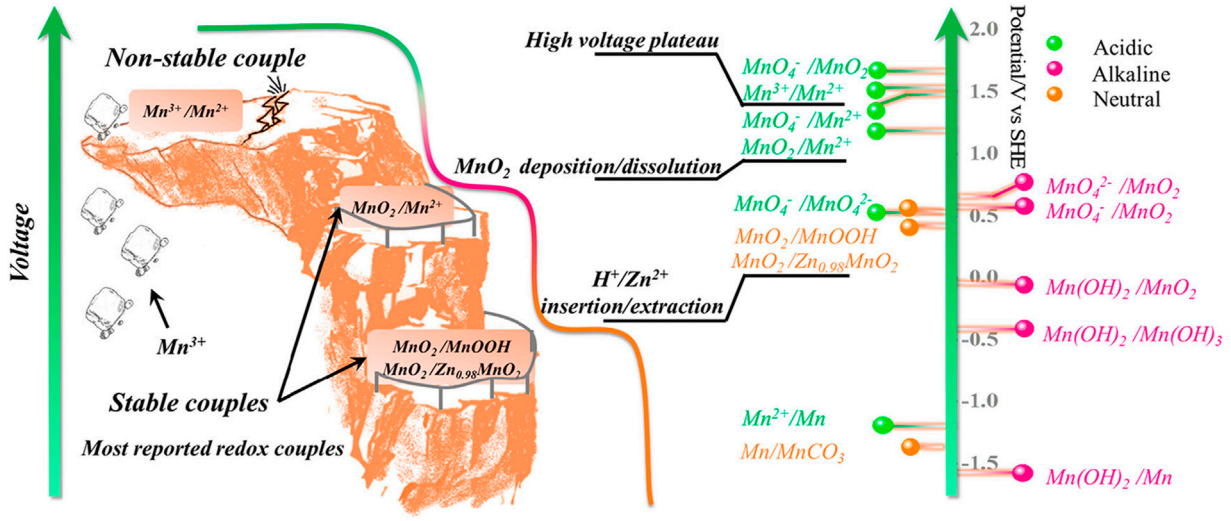

FIGURE 1
Schematic of various Mn redox couples with different redox potentials. Reproduced with copyright from ACS (Li et al., 2023).

electrolyte. This inefficiency resulted in capacitor breakdown after a few hundred cycles in the coin-cell setup.

Nevertheless, the use of the beaker-cell setup with a large electrolyte volume enabled a superior cycling performance of up to ~5,000 cycles. In 2012, the same group conducted an extended investigation on the limitations of the proposed system (Perret et al., 2012). The authors confirmed that the *in situ* electrochemical deposition/dissolution of MnO_2 is observed between 1.08–1.18 V and 1.09–1 V, respectively.

Additionally, they observed that the reversible solid-MnO_2 conversion to soluble-Mn^{2+} (1 cycle) is observed within a short period of 300 s. Furthermore, they revealed that the proportion of electrolyte volume to electrode mass is critical for the cycling stability of the system. Most importantly, they observed that the poor electrodeposition vs. deposition efficiency of MnO_2 altered the pH of the electrolyte and reduced the Mn^{2+} concentration in the repeated charge/discharge cycles; this eventually affected the final energy and power supplied by the system. Overall, various MOR processes may occur at different potentials, depending on the pH of the electrolyte, as illustrated in Figure 1 (Li et al., 2023). To enable reversible and high-energy Mn-redox chemistry, neutral or acidic electrolytes and high-potential redox couples are preferred. Thermodynamically, MnO_2/Zn_xMnO_2 and MnO_2/MnOOH couples proceed at ~0.5 V vs. the standard hydrogen electrode (SHE) in a neutral electrolyte and involve the intercalation of Zn^{2+} and H^+, respectively. In reality, the transformation of MnO_2 into Zn_xMnO_2 (charging) was observed to proceed at ~0.84 V vs. SHE in a 1 M $ZnSO_4$ electrolyte (Alfaruqi et al., 2015). Similarly, the reaction of MnO_2 into MnOOH was observed to occur at ~0.86 V vs. SHE in a 1 M $ZnSO_4$ electrolyte (Pan et al., 2016).

At high redox potentials of ~1.22 V vs. SHE, MnO_2/Mn^{2+} dissolution/deposition reaction proceeded in acidic electrolytes. Nevertheless, MnO_2 deposition was observed at ~0.84 V vs. SHE in a 2 M $ZnSO_4$/0.24 M $MnSO_4$ electrolyte (Zhao et al., 2018). To increase the redox potential further, Li et al. (Li et al., 2023) recently planned a strategy to promote Mn^{3+}/Mn^{2+}redox by increasing the acidity of the electrolyte beyond that of commonly reported electrolytes. In a 3 M H_2SO_4/0.5 M $MnSO_4$/0.1 M $SnSO_4$/0.05 M $Na_4P_2O_7$ electrolyte, they observed Mn^{2+} to Mn^{3+} oxidation at a high potential of ~1.67 V vs. SHE, which is slightly higher than the thermodynamic redox potential of ~1.5 V vs. SHE. In another study, Mn^{3+}/Mn^{2+} redox was reported by Wu et al. (Wu et al., 2022), who employed a catholyte containing 0.1 M $MnSO_4$, 1 M H_2SO_4, and 1 M HCl, in which the presence of HCl promoted the formation of soluble Mn^{3+} in the form of $[MnCl_4(H_2O)_2]$. Therefore, by summarizing the origin and evolution of this unique Mn deposition/dissolution chemistry, we understood the challenges and strategies for future research directions.

4 Mn deposition/dissolution chemistry and its contribution to the capacity outputs of Mn-based cathodes in ZIBs

Intercalation chemistry has been accepted worldwide after the successful commercialization of LIBs. Thus, Zn/$ZnSO_4$/α-MnO_2 rechargeable cells were established as rocking-chair-type batteries by Xu et al. (Xu et al., 2012) based on the Zn^{2+}-shuttling-mechanism model in the MnO_2 positive electrode, which indicated that the succeeding Mn-type cathodes in mild aqueous Zn cells can be categorized as intercalation cathodes for ZIBs. After the authors coined the term ZIB, an increasing number of studies have been published in this field.

Various polymorphs of MnO_2, including β-MnO_2, δ-MnO_2, λ-MnO_2, γ-MnO_2, and ε-MnO_2 have been documented as ZIBs that exhibit the Zn^{2+} shuttling mechanism; however, the electrochemical cycling stabilities of these ZIBs are unconvincing (Lee et al., 2013; Yuan et al., 2014; Islam et al., 2017; Mathew et al., 2020; Soundharrajan et al., 2020). Similar to other MnO_2-based rechargeable systems exhibiting common intercalation mechanisms, the Jahn-teller-distortion-induced Mn^{2+} dissolution was predicted to be the main reason for the downfall of ZIBs

containing Zn/MnO_2 polymorphs, which resulted in irreversible structural transformations, in mild aqueous electrolytes. Hence, to overcome this issue, the pre-inclusion of Mn^{2+} ions in the form of $MnSO_4$ in the $ZnSO_4$ electrolyte to maintain the ambient equilibrium conditions suggested by Pan et al. (Pan et al., 2016). When employing this strategy, the authors expected that MnO_2 was converted into MnOOH via the reversible H^+ intercalation/de-intercalation mechanism. Various research groups proposed various reaction chemistries in the following years concerning Mn^{2+}-comprising $ZnSO_4$ aqueous electrolytes for ZIBs. Based on this aspect, a detailed analysis of the electrochemical mechanism in MnO_2 cathodes was comprehensively summarized by Sambandam et al. (Sambandam et al., 2022) and Yang et al. (Yang et al., 2023).

Initially, Sun et al. (Sun et al., 2017) proposed a distinctive H^+/Zn^{2+} co-intercalation mechanism in Zn/MnO_2 systems. Interestingly, Li et al. (Li et al., 2019) planned the probability of intercalation-induced chemical conversions. More specifically, Lv et al. (Lv et al., 2022) proposed that during discharging, H^+/Zn^{2+} intercalation proceeds first, followed by the disproportionation of Mn^{3+}, resulting in the formation of Mn^{2+}. Whereas, Huang et al. (Huang Y. et al., 2019) reported a complex Zn-storage mechanism involving the participation of Zn^{2+}, H^+, and Mn^{2+} in Zn/MnO_2-based ZIBs in an Mn^{2+}-containing $ZnSO_4$ electrolyte. The complex reaction mechanism comprising intercalation, conversion, and Mn^{2+} oxidation proposed by the authors further added to the bulletin of reaction mechanisms for Zn/MnO_2-based ZIBs in an Mn^{2+}-containing $ZnSO_4$ electrolyte. Thus, in addition to the Zn^{2+} shuttling mechanism, several reaction mechanisms have been proposed for ZIBs in an Mn^{2+}-comprising $ZnSO_4$ aqueous electrolyte.

In particular, Beoun Lee et al. (Lee et al., 2016) claimed that only the reversible Mn^{2+} dissolution/MnO_2 deposition from the cathode material in a $ZnSO_4$ electrolyte and not the conventional Zn^{2+} (de) intercalation chemistry is the primary capacity donor (Eq 1).

$$3MnO_2 + 8Zn^{2+} + 2SO_4^{2-} + 16H_2O + 6e^- \leftrightarrow 3Mn^{2+} + 2Zn_4(OH)_6(SO_4)\cdot 5H_2O \quad (1)$$

More specifically, Mn^{2+} dissolves during the discharge process along with the *in situ* precipitation of $Zn_4(OH)_6(SO_4).5H_2O$ (ZHS), whereas the dissolved Mn^{2+} ions are re-deposited as MnO_2 during re-charging, and ZHS dissolves into the electrolyte in the Zn/α-MnO_2 ZIBs constructed by the author. The authors verified the reaction chemistry via *in situ* pH monitoring, by which they observed the reversible variation in pH during the charge/discharge process driven by the Mn^{2+} dissolution/MnO_2 deposition chemistry inside Zn/MnO_2 ZIBs. Additionally, from the *in situ* X-ray diffraction (XRD) analysis, the authors did not find any evidence of Zn^{2+} intercalation, whereas the reversible formation/dissolution of ZHS was a exceeding observation. The formation of ZHS was reported as an inevitable parasitic reaction in ZIBs containing a $ZnSO_4$ electrolyte in the following years, irrespective of the choice of cathode materials (Islam et al., 2017; Sambandam et al., 2018a; 2018b).

The addition of Mn^{2+} ions was primarily claimed to be a structural stabilizer in the early versions of ZIBs; however, the electrochemical activity of Mn^{2+} ions contributing to the energy output is accepted in modern-day ZIBs. Beoun Lee et al. (Lee et al., 2016) claimed that MnO_2/Mn^{2+} chemistry was the primary capacity contributor in Mn-based ZIBs in a $ZnSO_4$ electrolyte. In the following years, collective classical (de)intercalation and MnO_2/Mn^{2+} chemistry were challenged as the capacity contributors in Mn-based ZIBs in an Mn^{2+}-containing $ZnSO_4$ electrolyte. For example, in 2018, Zhao et al. (Zhao et al., 2018) reported that ZHS critically influences Zn/MnO_2-based ZIBs in an Mn^{2+}-containing $ZnSO_4$ electrolyte. To verify this, they directly used ZHS as the cathode material to emulate Zn/MnO_2-based ZIBs. Interestingly, the authors found that the Mn^{2+} ions consume ZHS in the 2 M $ZnSO_4$ + 0.24 M $MnSO_4$ electrolyte during the first charging process, generating MnO_2 *in situ*, as per the following reaction (Eq 2).

$$3Mn^{2+} + 2Zn_4(OH)_6SO_4\cdot 5H_2O \leftrightarrow 3MnO_2 + 2SO_4^{2-} + 8Zn^{2+} + 16H_2O + 6e^- \quad (2)$$

Although the authors did not account for the availability of additional Mn^{2+} ions in the electrolyte to encourage *in situ* MnO_2 deposition during subsequent cycles, they claimed that *in situ* MnO_2 deposition was followed by conventional intercalation mechanisms in the following charge/discharge cycles in Zn/MnO_2-based ZIBs, i.e., the two-step reversible redox reactions of Mn^{2+} shown in Eqs. 3, 4.

$$6Mn^{2+} + 4Zn_4(OH)_6SO_4\cdot 5H_2O \leftrightarrow 3ZnMn_2O_4 + 4SO_4^{2-} + 32H_2O + 13Zn^{2+} + 6e^- \quad (3)$$

$$7ZnMn_2O_4 + (5+2x)H_2O \leftrightarrow Zn_xMn_7O_{13+y}\cdot 5H_2O + (7-2x)Zn^{2+} + 4xH^+ + 6e^- \quad (4)$$

Although they observed the *in situ* deposition of MnO_2 from the ZHS cathode in the first cycle, they did not consider the reversibility of the *in situ* deposition of MnO_2 despite observing the *in situ* ZHS formation/dissolution during subsequent cycles. More specifically, Guo et al. (Guo et al., 2020) proposed that reversible Mn^{2+} dissolution/MnO_2 deposition is the dominant capacity supplier in the Zn/MnO_2-based ZIBs with a Mn^{2+}-containing $ZnSO_4$ electrolyte. They observed that the H^+/Zn^{2+} (de)intercalation reaction contributed the least to the capacity supplied by Zn/MnO_2-based ZIBs. With the help of sophisticated synchrotron X-ray experiments, including XRD, X-ray absorption spectroscopy, X-ray nano-tomography, and X-ray fluorescence microscopy, Kankanallu et al. (Kankanallu et al., 2023) further confirmed that the (de)intercalation process is absent in Zn/MnO_2 batteries. They explained that two types of Zn-Mn complexes, i.e., an amorphous Zn-Mn complex and a poorly crystalline $ZnMn_2O_4$ phase, are formed in the amorphous ZHS precipitate. The former can be reversibly dissolved in the electrolyte, contributing to the discharge capacity together with the dissolution of MnO_2, whereas the latter is found to be irreversible. The authors attributed the capacity fade to the build-up of the irreversible $ZnMn_2O_4$ phase upon cycling. Mn deposition/dissolution chemistry with zinc metal as anode are listed in (Table 1).

5 Cathode-free Zn/MnO_2 batteries with electrolyte additives

In addition to the direct usage of solid-MnO_2 as an active material for Zn/MnO_2 batteries involving charge-storage

TABLE 1 Batteries with Mn deposition/dissolution chemistry with metallic Zn as an anode.

S. No.	Cathode	Anode	Electrolyte	Capacity retention (%) (per cycle)	Current density (mA g^{-1})	Capacity (mA h g^{-1})	Voltage (V)
Zhang et al. (2020a)	LCMO (La-Ca co-doping MnO_2)	Zn foils	1 M $ZnSO_4$+0.4 M $MnSO_4$	76.8 (200)	0.2 A g^{-1}	297.3	0.8–1.9
Moon et al. (2021)	MnO_2/Mn^{2+}	Zn metal foil	2 M $ZnSO_4$+0.1 M $MnSO_4$	93 (2)	15.4	246	1.0–1.85
Lv et al. (2022)	Graphite foils	Zn foils	3 M $ZnCl_2$+0.1 M $MnCl_2$	58 (5,000)	8 mA cm^{-2}	550	1.2–1.4
Chen et al. (2021)	MnO_2	Zn metal foil	1 M $Zn(Oac)_2$+40 M KOAc-PAA)	82.7 (2000)	5 C	249.4	2
Zheng et al. (2021)	Carbon felt	Zn foils	3 M $MnSO_4$+0.84 M $ZnSO_4$+1.41 M $ZnBr_2$	94 (600)	20 C	950	1.98
6Liu et al. (2020b)	MnO_2	Zn metal	2 M $ZnSO_4$+0.2 M $MnSO_4$	90 (1,000)	0.5 A g^{-1}	415	1.0–2.0
Liu et al. (2021b)	MnO_2	Zn metal	0.2 M Hac	N/A (2000)	N/A	0.8 mA h cm^{-2}	1.8–2.0
Shen et al. (2021b)	MnO_2	Zn foil	ABC-H	99.54 (2000)	1 A g^{-1}	235	0.8–2.0
Mateos et al. (2020)	MnO_2	Zn foils	$ZnSO_4$+$MnSO_4$	1,000 s	1.6 A g^{-1}	450	N/A
Chen et al. (2021a)	Carbon nanotube	Zn foils	2 M $ZnSO_4$+0.2 M $MnSO_4$	17 (40)	0.2 A g^{-1}	110	1.6–1.8
Shen et al. (2021a)	MnO_2/CNT	Zn foils	2 mol L^{-1} $ZnSO_4$+0.005 mol L^{-1} $MnSO_4$	83.5 (2,500)	19.5 A g^{-1}	430	1.0–1.8
Huang et al. (2020a)	MnO_2/PPy	Zn metal foil	2 M $ZnSO_4$+0.1 M $MnSO_4$	91.6 (50)	100	256	0.8–1.8
Guo et al. (2020)	MnO_2/ZHS	Zn foils	$ZnSO_4$+$MnSO_4$	77 (50)	100	96.8	0.8–1.8
Liang et al. (2021)	MnO_2/GNS	Zn plate	2 M $ZnSO_4$+0.1 M $MnSO_4$	98 (3,000)	6 C	196	1.0–1.8
Islam et al. (2021)	ZnO-MnO@C	Zn	2 M $ZnSO_4$+0.2 M $MnSO_4$	84 (2000)	3,000	194	0.8–1.9
Dai et al. (2021)	CMO	Zn@CC	2 M $ZnSO_4$+0.5 M $MnSO_4$	93.2 (4,000)	10 mA cm^{-2}	589.6	1.5
Balland et al. (2021)	MnO_2	Zn	1.3 M $Al(OTf)_3$+0.3 M $Zn(OTf)_3$+0.3 M $MnCl_2$)	99.5 (1,400)	10 A g^{-1}	560	1.65
Huang et al. (2021)	MnO_2	Zn	1 M $MnSO_4$+1 M H_2SO_4	95.9 (100)	500 mA cm^{-2}	0.93 mAh cm^{-2}	0.6–2.0
Wu et al. (2021)	MnO_2	Zn foils	1 M $ZnSO_4$+0.2 M $MnSO_4$	70 (2000)	0.3 A g^{-1}	108	0.7–1.9
Chuai et al. (2021)	Carbon felt	Zn foils	0.09 M $CoSO_4$+0.06 M $NiSO_4$+1 M $MnSO_4$	90 (600)	10 C	10 mAh cm^{-2}	2.2
Huang et al. (2022)	Carbon felt-Mn_3O_4/$[Mn(NH3)_6]^{2+}$	Zn foil-Zn/$[Zn(NH_3)2(H_2))_4]^{2+}$	HCDCE	N/A (4,500)	2 mA cm^{-2}	1 mAh cm^{-2}	1.6
Zhang et al. (2020b)	MnO_2	Zn Plate	2 M NH_4Cl+0.2 M $ZnCl_2$+0.02 M $MnSO_3$	63.2	1 mA cm^{-2}	488.6	1.2–1.9
Naresh et al. (2021)	MnO_2	Zn	2 M $ZnSO_4$+2 M $MnSO_4$+1 M KCl	72 (100)	20 mA cm^{-2}	N/A	1
Zhong et al. (2022)	δ-MnO_2	Zn metal foil	2 M $ZnSO_4$+0.4 M $MnSO_4$	0 (50)	100	339.5	1.0–1.8

(Continued on following page)

TABLE 1 (*Continued*) Batteries with Mn deposition/dissolution chemistry with metallic Zn as an anode.

S. No.	Cathode	Anode	Electrolyte	Capacity retention (%) (per cycle)	Current density (mA g^{-1})	Capacity (mA h g^{-1})	Voltage (V)
Liu et al. (2022b)	MnO_2	Zn	0.5 M $ZnCl_2$+0.5 M $Mn(Ac)_2$+2 M KCl+1.75 M Hac	81.06 (2000)	50 mA cm^{-2}	5 mAh cm^{-2}	1.0–2.0
Lei et al. (2021)	Carbon felt-MnO_2	Carbon felt-Zn	1 M $Mn(Ac)_2$+1 M $Zn(Ac)_2$+2 M KCl	0 (225)	N/A	50 mA h cm^{-2}	20
Xu et al. (2023)	Carbon cloth	Zn foil	Three phase electrolytes	95 (350)	5 C	610	1.0–3.0
Shen et al. (2021a)	MnO_2/CNT	Zn	$ZnSO_4$+$MnSO_4$	83.5 (2,500)	10 mA cm^{-2}	430	1.0–2.0
Lv et al. (2022)	Graphite foil (MnO_2)	Zn foil	3 M $ZnCl_2$+0.1 M $MnCl_2$	0 (5,000)	16 mA cm^{-2}	550	1.8
Liu et al. (2021a)	Fluorine doping MnO_2	Zn foil	2 M $ZnSO_4$+0.1 M $MnSO_4$	100 (1,200)	5 C	103 mAh/g	0.8–1.8
Liang et al. (2021)	α-MnO_2	Zn Plate	2 M $ZnSO_4$+0.1 M $MnSO_4$	98 (3,000)	6 C	272	1.0–1.8
Kim et al. (2023)	MnO_2	Zn	0.2 M $ZnSO_4$+2.0 NaOH	0 (100)	10 mA/cm^2	550	2.3–2.4
Liu et al. (2023)	α-MnO_2	Zn foil	3 M $ZnSO_4$	94 (300)	0.1 A g^{-1}	323	1.8–2.2
Kankanallu et al. (2023)	β- MnO_2	Zn	2 M $ZnSO_4$ + 0.1 M $MnSO_4$	NA	C/5	150	1–1.75
Sun et al. (2022)	MnO_2	Zn	1 M $MnSO_4$/1 M $ZnSO_4$/ 0.1 M H_2SO_4	83.6 (1,000)	5 C	445	1.95
Deng et al. (2023)	MnO_2	Zn	2 M $ZnSO_4$ and 0.5 M $MnSO_4$	100 (800)	0.5 mAh cm^{-2}	570	1.95
Liu et al. (2022b)	MnO_2	Zn	1.75 M HAc	81.06 (2000)	50 mA cm^{-2}	5 mAh cm^{-2}	1.30–2.35

mechanisms with partial deposition/dissolution chemistry, cathode-free Zn/MnO_2 batteries driven by the direct participation of deposition/dissolution chemistry have recently attracted attention from energy researchers.

In cathode-free Zn/MnO_2 batteries, conducting carbon can be used as a cathode instead of solid MnO_2, with a metallic Zn anode. During charging, MnO_2 (Eq 5) and Zn deposition (Eq 6) proceed on the cathode and anode, respectively (Liu et al., 2020b; Aguilar et al., 2022).

$$Mn^{2+}_{(aq)} + 2H_2O \rightarrow \varepsilon - MnO_{2(s)} + 2e^- + 4H^+_{(aq)} \quad (5)$$

$$Zn^{2+}_{(aq)} + 2e^- \rightarrow Zn_{(s)} \quad (6)$$

However, cathode-free Zn/MnO_2 batteries lose substantial capacity owing to the incomplete dissolution of MnO_2 (under high areal capacities) and the poor electronic conductivity of the deposited MnO_2.

Notably, the electrolyte is crucial in promoting the reversible Mn^{2+}/MnO_2 reaction to ensure the long life of a Zn/MnO_2 battery. Recently, considerable research efforts have been targeted toward improving the reversibility of Mn^{2+}/MnO_2 reactions in Zn/MnO_2 batteries. For example, Xinhua Zheng et al. (Zheng et al., 2021) used Br as a redox mediator to enhance the chemical dissolution of over-deposited MnO_2, thereby preserving the reversibility of Mn^{2+}/MnO_2 deposition/dissolution.

The authors validated that the presence of Br^- in the electrolyte is directly involved in the dissolution of over-deposited MnO_2 on carbon felt based on the following reaction: Eqs. 7, 8

$$MnO_2 + 4H^+ + 3Br^- \leftrightarrow Mn^{2+} + Br_3^- + 2H_2O \quad (7)$$

$$Br_3^- + 2e^- \leftrightarrow 3Br^- \quad (8)$$

The authors claimed that 1/3 of the MnO_2/Br_2-Zn battery capacity mainly originated from the electrochemical conversion of Br^{3-} to Br^- via a redox reaction. Furthermore, from the *ex-situ* XRD analysis, the Br mediator was found to enhance the reversibility of MnO_2/Mn^{2+} reactions in the MnO_2/Br_2-Zn battery (Figure 2). The designed MnO_2/Br-Zn battery revealed a high discharge voltage of 1.98 V with an aerial capacity of 5.8 mAh cm^{-2}. More importantly, the MnO_2/Br-Zn battery exhibited long-term stability with 100% capacity retention for 600 cycles at a 20 C rate. Furthermore, the authors scaled up a MnO_2/Br_2-Zn battery to obtain a large capacity of 1,200 mAh and a potential energy density of 32.4 Wh kg^{-1}. The imperative highlight of this study is the practically feasible low-energy cost under 15 US$ kWh^{-1}, which is highly beneficial for the large-scale energy-storage market.

Lei et al. Lei et al. (2021) used a redox mediator to facilitate MnO_2 dissolution and enhanced cyclic stability by recovering the lost capacity from exfoliated MnO_2 layers. The authors used iodine as a redox mediator (0.1 M KI), as it has a suitable potential (0.536 V

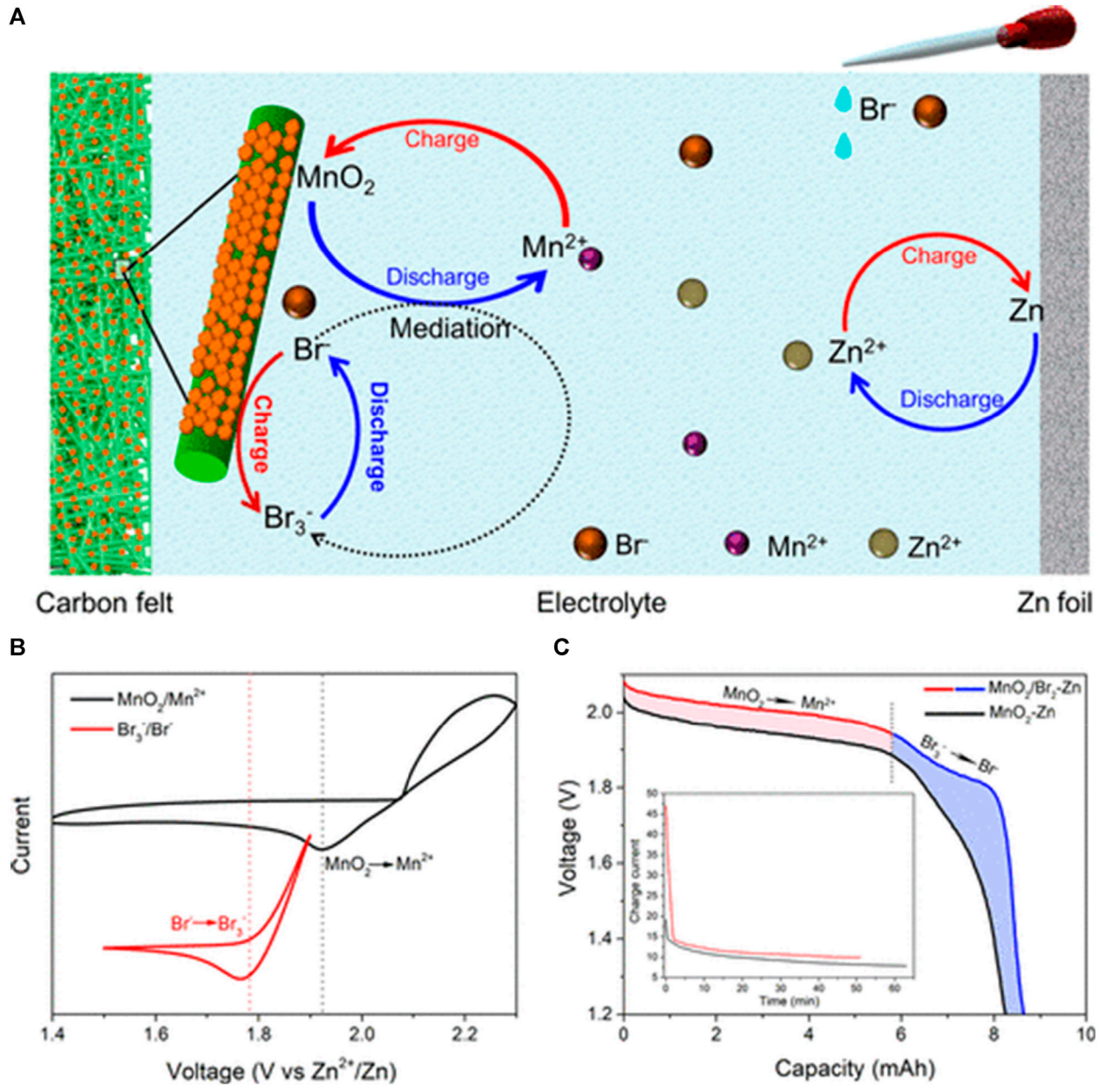

FIGURE 2
(A) Schematic illustration of a cathode-free MnO_2/Br_2-Zn battery. **(B)** CV curves involving Br^{3-} to Br^- redox and Mn^{2+}/MnO_2 redox reactions. **(C)** Discharge curves of the MnO_2/Br_2-Zn and MnO_2/Zn battery. Reproduced with copyright from ACS (Zheng et al., 2021).

vs. SHE) with high reversibility and fast kinetics. They reported the working mechanism of the KI mediator for facilitating MnO_2 dissolution as follows (Lei et al., 2021):

$$I_2 + 2e^- \rightarrow 2I^- \quad (9)$$

$$3MnO_2 + 3I^- + 4H^+ \rightarrow Mn^{2+} + I_3^- + 2H_2O \quad (10)$$

$$I_3^- + 2e^- \rightarrow 3I^- \quad (11)$$

During the discharging process, I^- chemically reacts with residual MnO_2 or exfoliated MnO_2 layers to form Mn^{2+} and produces I_3^-. Subsequently, I_3^- is electrochemically reduced to I^-, which continues to consume the remaining dead MnO_2. This process prevents the accumulation of dead MnO_2 and the insertion of H^+, thereby increasing the Coulombic efficiency and capacity of the battery. The authors confirmed the reaction between I^- and MnO_2 (Equation 10) using ultraviolet-visible spectroscopy. The two peaks at 289 nm and 351 nm in the spectra correspond to I_3^-. The triiodide crossover (I_3^-) was reported to be retarded due to the formation of solid I_2, which does not react with MnO_2, during the charging process. Generally, the mediator reaction is driven by the lower redox potential of the mediator than that of Mn^{2+}/MnO_2. The author explained this via charge-discharge voltage profiles, in which at a discharge potential of >1.45 V, regular MnO_2 dissolves to form Mn^{2+} until the potential reaches the reduction potential of I_2 to I^-. At potentials <1.45 V, the mediator reaction occurs according to Eq 9, and this process continues until all the MnO_2 is consumed. By deploying this

strategy to the Zn-Mn battery, the authors achieved stable cyclic stability of over 400 cycles at 2.5 mA/cm^2. Further, they designed Zn-Mn redox-flow batteries and achieved stability of 225 cycles at 15 mA/cm^2 and more than 50 cycles at a high areal capacity of 50 mA/cm^2, which is the highest among those of the reported Zn-Mn batteries. A similar approach to improve performance through the addition of a redox mediator was reported by Liu et al. (Liu et al., 2022b). They demonstrated that the addition of $CrCl_3$ to the electrolyte may reduce suspended MnO_2. Therefore, their Zn-MnO_2 cell with a modified electrolyte could deliver a stable cycling performance for 500 cycles, delivering ~0.4 mAh cm^{-2} at 10 mA cm^{-2}, whereas the cell without $CrCl_3$ stopped working after <100 cycles.

In another report, Liu et al. (Liu et al., 2021b) studied the reaction mechanism of the Zn-MnO_2 battery and its relationship with the pH of the electrolyte by substituting the H_2SO_4 additive with CH_3COOH. They suggested that a dual mechanism occurs in the Zn-MnO_2 battery, which includes 1) dissolution and deposition of MnO_2 and 2) (de)intercalation of H^+ and Zn^{2+} into residual MnO_2. They conducted X-ray photoelectron spectroscopy (XPS) analysis to confirm the presence of a dual Zn^{2+} and H^+ intercalation mechanism in the Zn-MnO_2 battery. Under low pH, dissolution and deposition of MnO_2 from the electrolyte is the primary reaction and not the (de)intercalation process. The drawback of using an H_2SO_4 additive is that its strong acidity causes corrosion and H_2 evolution reactions at the Zn anode.

Additionally, further intercalation of H^+ increases the pH of the electrolyte, retarding the dissolution of MnO_2 during the discharge process. The buffering effect of the added CH_3COOH reduces the fluctuation phenomenon and, therefore, increases cyclic stability. They assembled a soft package battery using an acidic CH_3COOH electrolyte with an Al plastic film and achieved a long lifetime of 2000 cycles with a Coulombic efficiency of 99.6%. The beneficial use of weak acids was additionally demonstrated by Mickaël et al. (Mateos et al., 2020). They conducted an in-depth quantitative spectro-electrochemical analysis of MnO_2 thin-films in unbuffered and buffered aqueous electrolytes of different natures, compositions, and pH values. The study demonstrated that nearly two-electron storage capacity of MnO_2 is accessible when a weak Bronsted acid, such as $[Zn(H_2O)_6]^{2+}$ or $[Mn(H_2O)_6]^{2+}$ complexes, is present at a sufficiently high concentration. Moreover, reversible MnO_2/Mn^{2+} dissolution and deposition can also be achieved.

Similarly, Zhong et al. (Zhong et al., 2022) highlighted the beneficial effects of the acetate ion (Ac^-) as an additive. They proposed that dissolution, deposition, and (de)intercalation contributed to the charge-storage mechanism in their Zn/MnO_2 cell, and the use of Ac^- increased the proportion of the reaction, which resulted in an increase in cell capacity from 221.1 mAh g^{-1} to 339.5 mAh g^{-1}. Accordingly, buffered electrolytes loaded with Mn^{2+} can yield high gravimetric capacity and stable voltages at the MnO_2 electrodes. A high gravimetric capacity of 450 mAh g^{-1} is obtained at a high rate of 1.6 A g^{-1}, with a Coulombic efficiency close to 100% and an MnO_2 utilization of 84%. This study revealed another interesting mechanism in mild aqueous electrolytes and clarified the benefit of buffered electrolytes for maximizing the performance of ZIBs (Mateos et al., 2020).

To prevent the irreversible side reaction involving Mn^{2+} dissolution, a pre-treatment with an artificial electrode microskin (EMS) was proposed and applied on the surface of an MnO_2 cathode

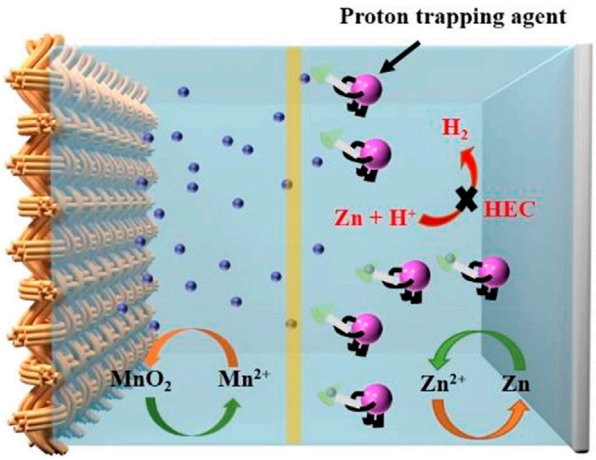

FIGURE 3
Schematic illustration of the working mechanism of the proton trapping agent. Reproduced with copyright from ACS (Sun et al., 2022).

(Liu et al., 2020b). The bionic EMS composed of C–H groups containing phenylalanine and tyrosine amino acids can effectively confine Mn^{2+} dissolution via a physical barrier and chemical adsorption. Therefore, the dissolved Mn^{2+} species are localized on the cathode surface owing to van der Waals forces, hydrogen bonding, and/or ionic bonding. Interestingly, the assembled aqueous Zn//δ-MnO_2 battery with a 10.1-μm microskin displayed a discharge capacity of 415 mAh g^{-1} at 20 mA g^{-1}. The cell exhibited relatively good capacity retention at low current densities but struggled at medium and high-rate operations. Notably, although adding an extra layer on the electrode surface can form a protective layer, the layer may partially passivate the movement of host ions (protons or Zn^{2+}), thereby reducing reaction rates. The results demonstrated a highly fluctuated cycling process at high reaction rates; however, the material strategies and cell components need further improvement.

Widening the potential window is the main challenge in achieving feasible ZIBs. The potential window is limited by the aqueous electrolyte in which the oxygen evolution reaction (OER) and hydrogen evolution reaction (HER) can proceed on the cathode and anode, respectively. Although the use of acidic electrolytes inhibits the OER on the cathode, the presence of H^+ promotes HER on the Zn anode (Xie et al., 2020). In theory, the concept of employing acidic and alkaline electrolytes separated by a neutral medium significantly extends the operating range up to 2.83 V, achieving a possible energy density of 1,621.7 Wh kg^{-1} in Zn-MnO_2 batteries (Zhong et al., 2020). However, the H^+ present in the catholyte may still migrate to the anolyte, resulting in irreversible HER on the anode. One strategy to suppress the impact of H^+ migration to the anolyte is to employ a proton trapping agent (PTA), as demonstrated by Sun. et al. (Sun et al., 2022). PTAs are a category of salts containing weak acidic ions, such as $H_2PO_4^-$, $C_6H_5O_7^{3-}$, and Ac^-, that are capable of trapping H^+, as shown in Figure 3. Sun. et al. (Sun et al., 2022) suggested that CH_3OO^- has the best ability to suppress HER, enabling the reversible plating and stripping of the Zn anode. They increased the lifetime of their Zn/MnO_2 cell 5-fold to 400 cycles by using 1 M $MnSO_4$ + 0.15 M H_2SO_4 + 0.1 M NaCl as the catholyte and

0.8 M $ZnSO_4$ + 0.2 M $Zn(COOH)_2$ + 0.1 M NaCl as the anolyte. The concept of electrolyte buffering can be applied by adding an electrolyte additive and by introducing a cathode additive that can attract protons during the MnO_2 deposition process (Eq 12). Using the cathode additive approach, Aguilar et al. (Aguilar et al., 2022) prepared a cathode composite consisting of 10 wt% $Mg(OH)_2$ and 90 wt% carbon. $Mg(OH)_2$ buffered the electrolyte by consuming protons during discharging (Eq. 12) and releasing them during charging (Eq 13). This approach suppressed the corrosion of the Zn anode during charging and promoted MnO_2 dissolution during discharging. Consequently, a stable cell performance with a discharge capacity of 412 mAh g^{-1} for 180 cycles was achieved (Aguilar et al., 2022).

$$Mg(OH)_{2(s)} + 2H^{+}_{(aq)} + 4H_2O \leftrightarrow [Mg(H_2O_6)]^{2+}\ pK_s = 11\ (\text{in pure water}) \quad (12)$$

$$[Mg(H_2O)_6]^{2+} \leftrightarrow [Mg(OH)(H_2O)_5]^{+} + H^{+}_{(aq)}\ pK_{a1} = 11.4\ (\text{in pure water}) \quad (13)$$

The use of Ac^{-} in a slightly different manner was reported by Chen et al. (Chen et al., 2021). They proposed an interesting approach of using an oversaturated gel electrolyte (OSGE) prepared by dissolving $Zn(CH_3CO_2)_2.2H_2O$ and CH_3CO_2K in deionized water with polyacrylic acid at 75 °C. This gel electrolyte provides an excellent solvation sheath, which is stable during the high-voltage operation of ZIBs. The OSGE-based Zn-MnO_2 battery retained 304 mAh g^{-1} capacity at 1 C with a limit in the range of 0.8–2.0 V after more than 100 cycles. The system could operate at high current densities of 10 C and achieved 82.7% capacity retention after 2000 cycles. Moreover, the system showed highly stable Zn deposition at room temperature while operating up to 2.0 V.

The high viscosity of the gel electrolyte demonstrates excellent compatibility with ZIBs, generating possibilities for new solid-electrolyte strategies. In a recent report, a novel tri-layer hydrogel electrolyte was prepared via multiple injection and molding steps to form three layers of polyacrylamide (PAM)/$ZnSO_4$, alkaline sodium polyacrylate (PAA-Na)/$ZnSO_4$, and PAM/$ZnSO_4$/H^{+} (Shen Z. et al., 2021). The two-electron redox of MnO_2/Mn^{2+} and anode protection are crucial for maintaining high battery performance.

The battery exhibits a high capacity of 516 mAh g^{-1} at 50 mA g^{-1} and excellent capacity retention of 93% at 5 A g^{-1} after 5,000 cycles. Moreover, owing to the flexible nature of the hydrogel, this solid electrolyte demonstrated outstanding mechanical stability while maintaining more than 99.4% capacity. This allowed the assembly of the fibrous Zn/MnO_2 battery with excellent flexibility, demonstrating the potential for use in wearable electronics.

A unique approach to improve the reversibility of the MnO_2/Mn^{2+} redox reaction through the regulation of the upper cut-off voltage (UCV) was proposed by Liu et al. (Liu et al., 2023). By increasing the UCV to 2.2 V, followed by a constant-voltage holding step during the first charge, the deposited MnO_2 participated in the two-electron reduction reaction from MnO_2 to Mn^{2+}. This activation originated from the contraction and formation of oxygen vacancies in the original MnO_2 cathode, forming weakly bonded MnO_2 deposits. The authors demonstrated that the modified charging protocol (2.2 V + hold vs. 1.8 V) in the Zn/MnO_2 cell with a 3 M $ZnSO_4$ electrolyte without Mn^{2+} increased capacity retention from 31.5% to 94.6% after 300 cycles. To protect the Zn anode from being corroded, Deng et al. (Deng et al., 2023) employed the concept of a nanomicellar electrolyte by adding methyl-urea (Mu) molecules to $ZnSO_4$/$MnSO_4$ electrolytes. The addition of Mu divided the aqueous solvent environment into hydrophilic and hydrophobic regions in which cations and anions were encapsulated by nanomicelles, as illustrated in Figure 4. The participation of Mu molecules in the solvation of Mn^{2+} and Zn^{2+} expels water molecules and decreases the desolvation energy barrier. Moreover, the nanomicelles enable a controllable release of Mn^{2+} and Zn^{2+}, facilitating uniform Zn deposition, as illustrated in Figure 4B.

The deposited Zn is further protected from water molecules by the *in-situ*-formed interphase layer comprising Zn_x $(Mu)_ySO_4$.nH_2O. With the use of 7 M Mu in a 2 M $ZnSO_4$ + 0.5 M $MnSO_4$ electrolyte, they operated the Zn/MnO_2 battery for 800 cycles with 100% capacity retention at 0.5 mAh cm^{-2}, whereas the cells without the Mu additive failed after 200 cycles. The authors also claimed that the improved cell has an average discharge voltage of 1.87 V, and they estimated that the battery has a specific energy of ~800 Wh kg^{-1} at the material level.

Overall, previous research on ZIBs has claimed that the capacity performance of Mn-based cathodes is mainly due to the active material of the cathode. As discussed in this section, more recent studies have confirmed that the dissolved Mn^{2+} ions, either from the cathode or in the form of electrolyte addition, are the main contributors to the capacity of the Mn deposition and dissolution in ZIBs. The contribution of Mn deposition/dissolution to the capacity performance of Mn-based cathodes for ZIBs is therefore very imperative. However, the lack of a comprehensive and practical protocol for differentiating capacity hinders the true capacity contribution when using manganese-based oxides as cathodes in ZIBs. Still, there is a strong interest in utilizing the use of Mn deposition/dissolution as a way to increase the capacity output of ZIBs has been overlooked by researchers. However, the consequences are amplified by the complexity of the reaction mechanism and the large volume expansion due to the uncontrollable gas evolution induced by the pH change associated with the addition of Mn^{2+}.

6 Advanced batteries based on Mn deposition/dissolution chemistry

6.1 Aqueous Mn flow battery (redox flow-battery)

Although vanadium redox-flow batteries dominate flow-battery research, the use of toxic and expensive vanadium restricts their practical applications. Hence, Mn redox chemistry has recently been proposed to construct hybrid-Mn flow batteries. For example, the design of a MnO_2/Mn^{2+} redox flow battery has been proposed by Lei. et al. (Lei et al., 2023), as shown in Figure 5A. The authors proposed the use of carbon felt and polysulfide-treaded Ni foam as the positive and negative electrodes, respectively. On the positive electrode, a MnO_2|Mn^{2+} redox couple was used, and on the negative electrode, S_2^{2-}|S^{2-} redox chemistry occurred. As a catholyte, a solution of 1 M $Mn(COOH)_2$ + 2 M KCOOH +2 M KCl +0.1 M KI was used, and as

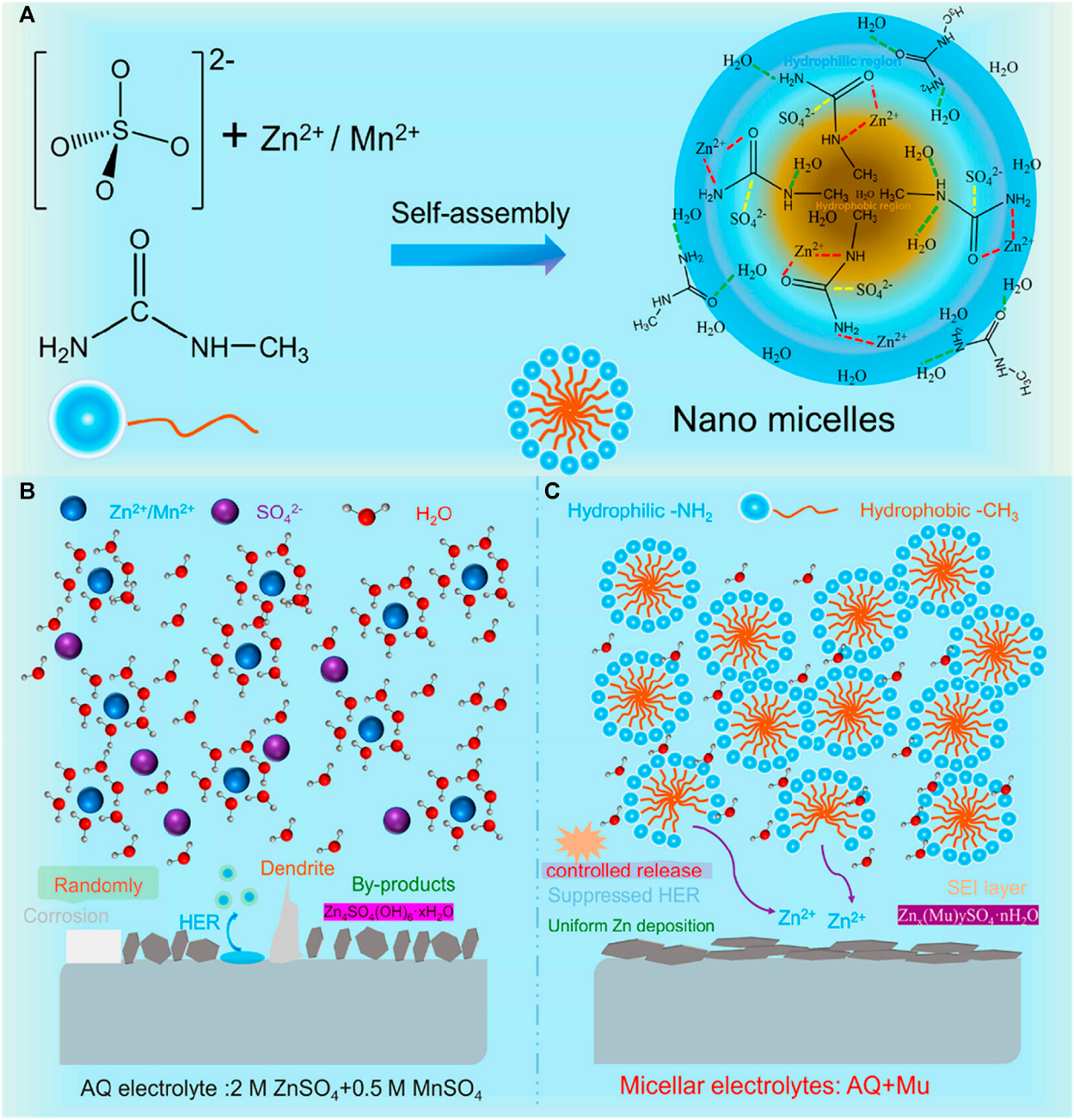

FIGURE 4
(A) Schematic illustration of the nanomicelle-electrolyte self-assembly and the Zn-plating processes in **(B)** aqueous (AQ) and **(C)** nanomicelle electrolytes. Reproduced with copyright from ACS (Deng et al., 2023).

an anolyte, a solution of 2 M K_2S_2 + 1 M KOH was employed. In the catholyte, $COOH^-$ was chosen as the counter anion owing to its buffering effect and higher stability than SO_4^{2-}. Furthermore, iodide was added to act as a discharge mediator, facilitating a more facile MnO_2 dissolution. Finally, to ensure high-performance stability, the catholyte and anolyte were separated by a charge-reinforced membrane to prevent polysulfide crossover. The authors demonstrated a negligible voltage-profile shift of the battery during cycling (Figure 5B), resulting in an impressive capacity retention of 98% after 75 cycles. They also suggested that the use of abundant Sulfur (S) and Mn could bring the cost of the electrolyte to \$11 kWh^{-1}.

Another redox-flow battery design was proposed by Kim et al. (Kim et al., 2023), who constructed a hybrid cell with three electrolyte chambers. This allowed the carbon felt anode to be operated in an anolyte with pH > 14, allowing for $Zn(OH)_4^{2-}$ reduction to Zn (−1.22 V vs. SHE), which has a lower redox potential than that of Zn^{2+} reduction (−0.76 V vs. SHE). Using the Ag-decorated carbon felt cathode operated in an acidic catholyte, reversible MnO_2/Mn^{2+} dissolution/deposition was achieved. Therefore,

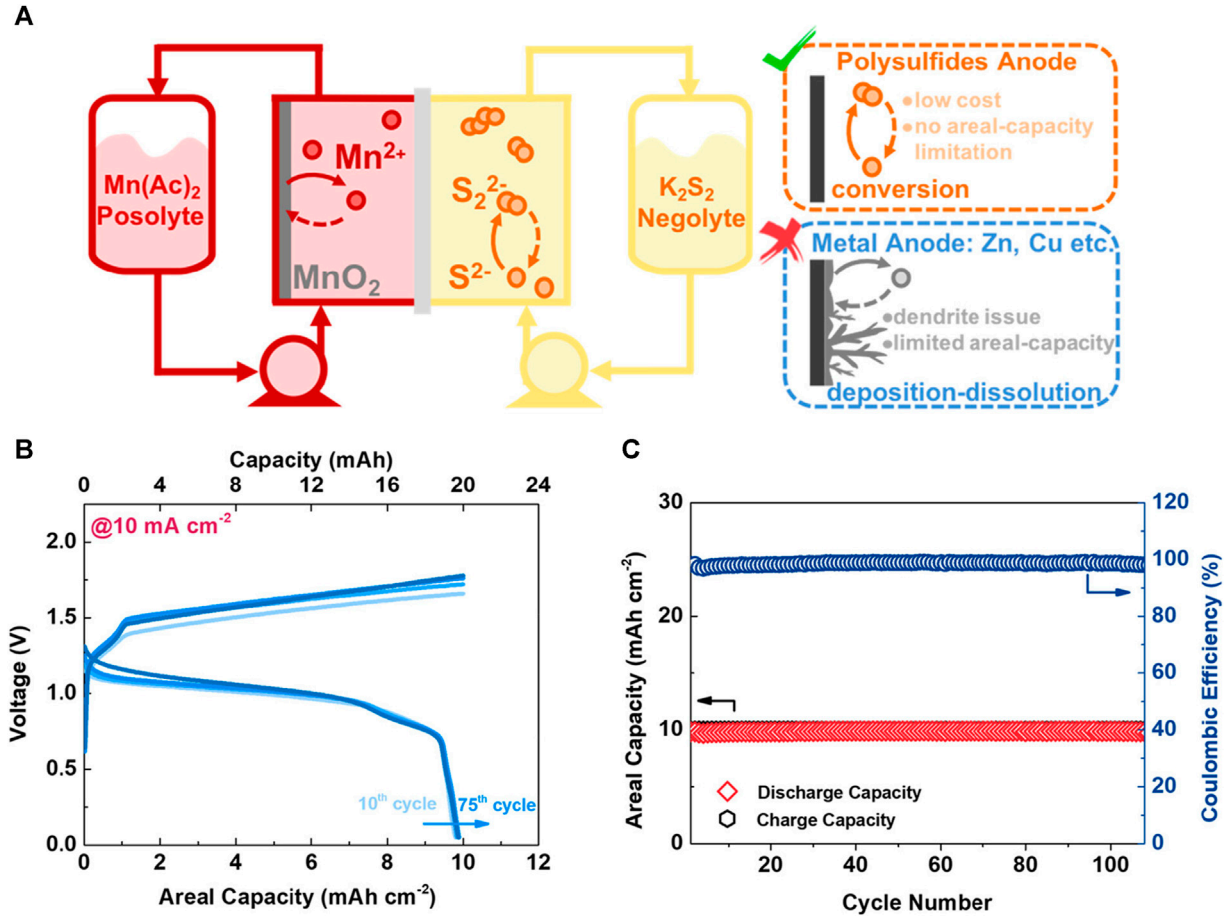

FIGURE 5
(A) Schematic illustration of the Sulfur-Mn (S-Mn) flow battery design. **(B)** Voltage profiles of the S-Mn flow cell operated at a current density of 10 mA cm^{-2}. **(C)** Comparison between the capacity retention of the S-Mn and Zn-Mn flow cells with a charging areal capacity of 50 mAh cm^{-2}. Reproduced with copyright from ACS (Lei et al., 2023).

the cell delivered a stable specific capacity of ~550 mAh g^{-1} and a discharge voltage of ~2 V after 100 cycles.

6.2 Aqueous Sn-Mn battery

In a recent study, Wei et al. (Wei et al., 2019a) constructed a new Sn-Mn battery by using non-toxic and low-cost metallic Sn as a negative electrode. More specifically, the positive (carbon felt) and negative (metallic Sn) electrodes were placed between transparent acrylic frames, and 0.5 $MnSO_4$ + 2.8 M H_2SO_4 and 0.3 M $SnSO_4$ + 2.8 M H_2SO_4 were filled separately as a catholyte and anolyte, respectively. The authors validated the occurrence of reversible Sn deposition/stripping reactions at the negative electrode and reversible *in situ* electrochemical deposition/dissolution of MnO_2 at the positive electrode via multiple *ex situ* probing techniques such as SEM, XRD, and XPS. The authors found that the proposed battery design delivered a maximum energy output of 86% at 30 mA cm^{-2}. Furthermore, the authors claimed that the high hydrogen overpotential (~0.13 V vs. SHE) of Sn minimized the parasitic reaction, thereby delivering stable energy efficiency (91.5%) and cycle life. Additionally, the authors recommended the use of electrolyte additives such as $TiOSO_4$ and methane sulfonic acid (MSA) to eliminate the Mn disproportionation reaction.

6.3 Aqueous Mn-Pb battery

The Pb-acid battery comprises $PbO_2|PbSO_4$ and $Pb|PbSO_4$ redox at the cathode and anode, respectively and has been dominating the stationary energy-storage market for more than two centuries. However, the inherent difficulties of the Pb-acid battery remain unsolved. In particular, on the positive electrode, PbO_2 exhibits poor kinetics related to the $PbO_2/PbSO_4$ conversion products, a high working potential, and uncontrollable volume changes, which collectively induce grid corrosion and peeling of the positive electrode. Additionally, sulfation at high-rate operations on the negative electrode is a primary issue, although innovative and practicable carbon additive approaches were found to be effective in alleviating the sulfation issue. Recently, Huang et al. (Huang et al., 2020b), constructed a new Mn-Pb battery by replacing the PbO_2 positive electrode with carbon felt and the H_2SO_4 electrolyte with an H_2SO_4 + $MnSO_4$ combination. The negative electrode, however, remained the same ($PbSO_4$). The new Mn-Pb battery employs a

hybrid working mechanism during operation, in which the reversible MnO_2/Mn^{2+} redox reaction proceeds at the positive electrode and the $PbSO_4/Pb$ redox reaction occurs on the negative electrode. The advantage of the newly designed Mn-Pb battery is its long cycle life of 10,000 cycles, high voltage of ~1.55 V, and high energy density of 187 Wh L^{-1}. The proposed Mn-Pb battery costs US$ 8.6 kWh^{-1}, which is comparable to other large-scale energy-storage batteries. Interestingly, the authors demonstrated another aspect of the Mn-Pb battery by formulating a flow-assisted Mn-Pb device comprising an electrochemical reaction box and electrolyte reserve tank. The flow-driven Mn-Pb battery achieved a stable cycle life of up to 500 cycles with a discharge capacity of 97.5 mAh. Although the authors claimed that Pb recycling is a mature technique, the use of toxic and hazardous Pb in this newly designed Mn-Pb system is a major hindrance to realizing large-scale devices.

Interestingly, Pb may also be used partially on the Zn anode as a protective layer, as demonstrated by Ruan et al. (Ruan et al., 2023). They introduced a Pb-containing (Pb and $Pb(OH)_2$) interface on the Zn anode that can readily react with an H_2SO_4-containing electrolyte to form $PbSO_4$, preventing direct contact between the electrolyte and the Zn anode. Furthermore, the addition of $Pb(CH_3COOH)_2$ to the electrolyte resulted in the formation of a $PbSO_4$ precipitate and the release of Pb^{2+} ions that can participate in Pb deposition during charging. The low affinity of Pb and $PbSO_4$ toward protons and strong Pb-Pb and Pb-Zn bindings increased the H^+ corrosion resistance of the Zn anode. With the use of the Zn-Pb anode in a 0.1 M H_2SO_4/1 M $ZnSO_4$/1 M $MnSO_4$/1 mg $Pb(CH_3COOH)_2$ electrolyte, the authors operated Zn/MnO_2 cells with a stable areal capacity of ~5 mAh cm^{-2} for 400 cycles, whereas the cell with a Zn foil only operated for <20 cycles.

6.4 Aqueous Na-Mn battery

Feng et al. (Feng et al., 2019) constructed a new aqueous Na-Mn hybrid battery (SMHB) by combining battery (Mn deposition/dissolution) and supercapacitor (Na^+ adsorption/desorption) chemistries. More specifically, the SMHB was constructed using a graphite-felt-based cathode (reversible conversion reaction of Mn^{2+} to MnO_2 prevailed) and activated-carbon-based anode (reversible Na^+ adsorption/desorption reaction was maintained), with a hybrid electrolyte (1 M Na_2SO_4 + 1 M $MnSO_4$ + 0.1 M H_2SO_4) combination. The designed SMHB system exhibited optimized electrochemical storage properties owing to the integrated merits of the supercapacitor and battery chemistries.

The SMHB supplied a high discharge voltage of 1.2 V, Coulombic efficiency of ~99.2%, and cyclic stability of 7,000 cycles. From the *ex situ* XRD and Raman analysis, the reversible deposition/dissolution of MnO_2/Mn^{2+} was verified. Interestingly, the authors compared the unique hybrid mechanism of the SMHB with the conventional Na^+ (de)intercalation mechanism in the purposefully designed $Na_{0.44}MnO_2$//activated carbon (AC) battery. From the electrochemical comparison, the authors found that the SMHB employing the hybrid mechanism exhibited faster kinetics than that of the $Na_{0.44}MnO_2$//AC battery employing the traditional Na^+ (de)intercalation mechanism. The authors claimed that SMHBs have great commercial value owing to the use of inexpensive and environmentally friendly resources.

6.5 Aqueous Cu-Mn battery

A novel Cu-Mn battery was developed by Wei et al. (Wei et al., 2019b) that uses inexpensive and readily available graphite felt as both the positive and negative electrodes placed separately inside a poly (methyl methacrylate) chamber. Both the electrode chambers were filled with a 0.8 M $CuSO_4$ + 0.8 M $MnSO_4$ + 0.8 M H_2SO_4 electrolyte separated using a Nafion 212 separator to prevent cross-contamination between the electrodes. The authors illustrated that the reversible Cu^{2+}/Cu (negative electrode) and Mn^{2+}/Mn^{3+} (positive electrode) redox chemistries are the potential capacity donors in the Cu-Mn battery. The authors verified that the Cu-Mn battery achieves an open circuit voltage close to 1.1 V. The newly designed Cu-Mn battery exhibited superior cycling stability with 79% capacity retention for more than 100 cycle tests at 10 mA cm^{-2}. The most significant advantage of the Cu-Mn battery is that the raw materials are readily available and inexpensive ($ 37.0 kWh^{-1}), which is superior to the well-established vanadium redox-flow battery ($ 116.4 kWh^{-1}). From impedance studies, the authors found that the Mn^{2+}/Mn^{3+} redox couple exhibited poorer diffusion kinetics than that of the Cu^{2+}/Cu redox couple. Hence, they recommended that energy researchers should focus on the catalytic activity of the Mn redox couple at the positive electrode instead of the Cu redox couple in the negative electrode, to improve the stability of the Mn-Cu battery.

6.6 Aqueous Mn-Bi battery

Liang et al. (Liang et al., 2019) formulated a MnO_2-Bi battery that can be sustained by the deposition-dissolution mechanism. The MnO_2-Bi battery achieved 80% Coulombic efficiency (CE) in acidic electrolytes, which is significantly lower than the CE of batteries with a Cu anode. The low CE can be attributed to the quasi-reversible plating and stripping of the Bi-metal in addition to the partial dissolution of MnO_2 during the discharging cycle. The quasi-reversible plating was further confirmed by the nonconformally placed Bi particles on the carbon-cloth electrode. The authors believe that the best way to improve battery performance is to select suitable and efficient electrolytes for deposition and dissolution with excellent efficiency. Yu et al. (Yu et al., 2021) developed a rechargeable alkali-acid Bi-MnO_2 hybrid battery with a Bi@C framework as the anode and a homemade MnO_2 cathode involving acidic (3 M $MnSO_4$ + 0.3 M H_2SO_4) and alkaline electrolytes (3 M NaOH) separated by anion and cation exchange membranes. The advantage of this decoupled Bi-MnO_2 battery is its high discharge voltage, long-term stability, and outstanding rate performance. Unlike the Ni-Bi battery, the Bi-MnO_2 battery provides an extraordinary specific power of 4900 W kg^{-1}, as well as a high specific energy of 156.2 Wh kg^{-1} (Yu et al., 2021a).

6.7 Aqueous Mn-Al battery

He et al. (He et al., 2019) recently demonstrated the use of a birnessite MnO_2 (Bir-MnO_2) cathode in high-energy aqueous Mn-Al batteries. The authors investigated the electrochemical behaviour of Bir-MnO_2 using a coin-cell configuration with 2 M aqueous aluminium trifluoromethanesulfonate ($Al(OTF)_3$) and Al-foils as

TABLE 2 Advanced batteries based on Mn deposition/dissolution chemistry with diverse metal anodes.

S. No.	Cathode	Anode	Electrolyte	Capacity retention (%) (per cycles)	Current density (mA g^{-1})	Capacity (mA h g^{-1})	Voltage (V)
Huang et al. (2020b)	MnO_2/Mn^{2+}	$PbSO_4/Pb$	1 M $MnSO_4$ + 0.5 M H_2SO_4	85 (45)	100 mA cm^{-2}	41.2 mAh cm^{-2}	1.55
Yang et al. (2020)	$MnCl_2$ (MnO_2/Mn^{2+})	$LaNi_5$ based Hydrogen storage (H)	2 M $MnCl_2$+0.1 M H_2SO_4	98 (130)	40	300	2.2
He et al. (2019)	Bir-MnO_2	Al foils (Al^{3+})	0.5 M $MnSO_4$	89 (65)	100	320	1.35
Huang et al. (2019a)	MnO_2/Mn^{2+}	Cu plate (Cu^{2+}/Cu)	H_2SO_4+$CuSO_4$+$MnSO_4$	73.7 (200)	10 mA cm^{-2}	50 mAh cm^{-2}	1.2
Wei et al. (2019b)	$MnSO_4$(Mn^{3+}/Mn^{2+})	$CuSO_4$(Cu^{2+}/Cu)	0.8 M $CuSO_4$+0.8 M $MnSO_4$+0.8 M H_2SO_4	79 (100)	10 mA cm^{-2}	7.5 Ah L^{-1}	1.1
Wei et al. (2019a)	0.5 M $MnSO_4$	0.3 M $SnSO_4$	2.8 M H_2SO_4	91.5 (100)	10 mA cm^{-2}	3.7 Ah L^{-1}	1.7
Yu et al. (2021)	MnO_2	Bi@C	3 M $MnSO_4$+0.3 M H_2SO_4 and 3 M NaOH	96 (9,500)	3 A g^{-1}	347.2	1.62
Liang et al. (2019)	MnO_2	Cu	0.3 M $CuSO_4$ + 0.3 M $MnSO_4$	68 (1800)	16 mA cm^{-2}	0.8 mAh cm^{-2}	1.2
Liu et al. (2020a)	Carbon felt (MnO_2-C)	Activated carbon (AC-AQS)	1 M H_2SO_4+1 M $MnSO_4$	99.9 (10,000)	50 mA cm^{-2}	0.796 mAh cm^{-2}	0.6–1.6
Oka et al. (2020)	MnO_2	pEP(NQ)E	1 M $MnSO_4$+0.05 M H_2SO_4	99 (50)	1 C	76 mAh/g	1
Wang et al. (2021)	MnO_2	Cd	0.5 M $CdSO_4$+0.5 M $MnSO_4$+0.5 M H_2SO_4	0 (20,000)	50 mA cm^{-2}	0.5 mAh cm^{-2}	1.12
Yu et al. (2022)	MnO_2	Sb/NCF (nitrogen doped carbon framework)	1 M KOH+ 0.054 M $C_8H_4K_2O_{12}Sb_2$	95	20 mA cm^{-2}	3.8 mAh cm^{-2}	1.6
Xu et al. (2022)	MnO_2	Al foils	1 M $AlCl_3$+1 M $MnCl_2$ in H_2O	0 (1,000)	2 mA/cm^{-2}	493 mAh/g	1.9
Li et al. (2023)	MnO_2	Sn	3 M H_2SO_4+0.5 M $MnSO_4$+0.1 M $SnSO_4$+0.05 M $Na_4P_2O_7$	58 (30,000)	5 mA cm^{-2}	533 mAh g^{-1}	1.6
Wu et al. (2022)	$MnSO_4$	$FeCl_3$	1 Mol L^{-1} HCl+ 1 Mol L^{-1} H_2SO_4	100 (280)	160 mA cm^{-2}	80.4 Ah L^{-1}	1.14
Ruan et al. (2023)	Ad//MnO_2	Zn@Pb	0.2 and 0.1 M H_2SO_4	99	8 mA cm^{-2}	1,000 mA h	1.9

the electrolyte and anodes, respectively. During discharge, Mn^{2+} dissolves into the electrolyte, and $Al_xMn_{(1-x)}O_2$ is formed, which works as a reversible cathode-active material in successive cycles. Here, Mn^{2+} was added to the electrolyte $MnSO_4$ to improve cycling performance. Additionally, the use of $AlCl_3$/1-ethyl-3-methylimidazolium chloride to remove the passive oxide layer on the Al surface was found to enhance cell performance. The authors observed a second-cycle discharge capacity of 554 mAh g^{-1} in the electrolyte with 0.5 M $MnSO_4$ at a current density of 100 mA g^{-1}. Under a discharge voltage of ~1.35 V, the specific energy was calculated to be 620 Wh kg^{-1}. This cell delivered 320 mAh g^{-1} after 65 cycles, whereas the cell without the $MnSO_4$ additive only delivered 42 mAh g^{-1} after 30 cycles.

6.8 Mn-H battery

Chen et al. (Chen et al., 2018) recently reported the design of rechargeable Mn-H batteries. The authors claimed these batteries are inexpensive, durable, and safe. This battery operates via the MnO_2/Mn^{2+} dissolution/deposition reaction on the cathode and catalytic hydrogen evolution/oxidation reactions on the anode. The Mn-H battery includes a cathode-less porous carbon felt, a glass fiber separator, a Pt/C catalyst-coated carbon felt anode, and an aqueous electrolyte containing Mn^{2+}. The authors implemented the Mn-H battery in custom-made Swagelok cells and performed electrochemical experiments in a 1 M $MnSO_4$ electrolyte at ambient conditions. They showed that the Mn-H battery

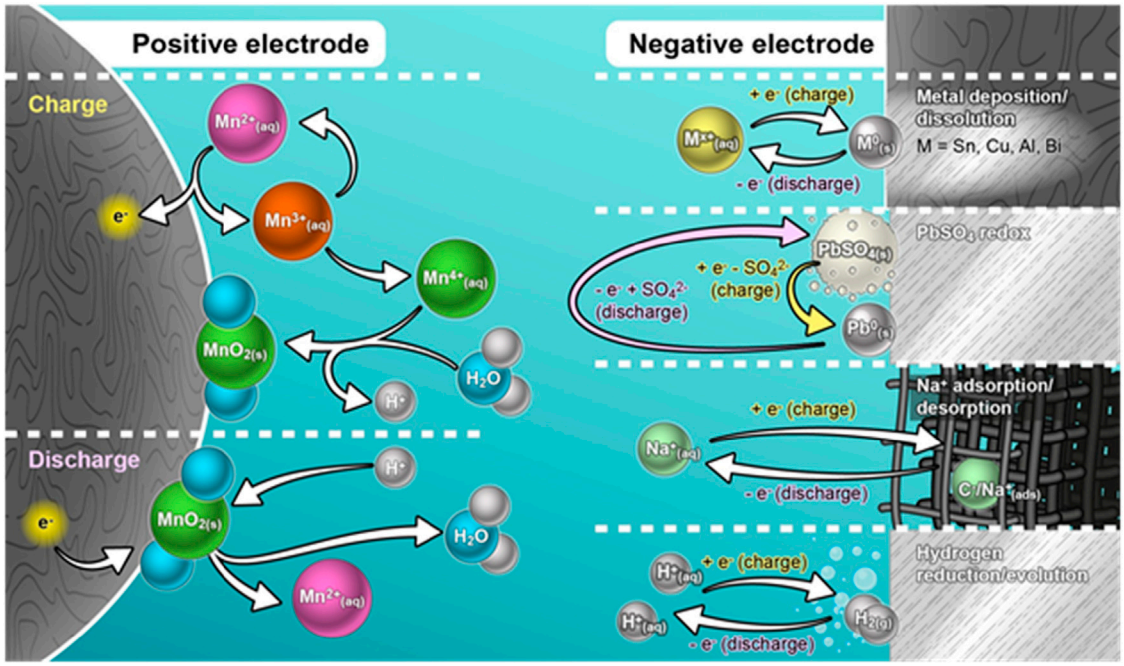

FIGURE 6
Schematic illustration of the underlying mechanism in the aqueous batteries involving MnO_2/Mn^{2+} redox couple associated with the different anode environments.

exhibited no detectable capacity degradation after 10,000 cycles at 1 mAh cm^{-2}. In a 4 M $MnSO_4$ electrolyte, the Mn-H battery delivered a specific energy and energy density of ~139 Wh kg^{-1} and ~210 Wh L^{-1}, respectively.

Furthermore, the author constructed a membrane-free cylindrical cell to demonstrate the scalability of the Mn-H battery. The cylindrical Mn-H battery has excellent long-term cycling stability with ~94.2% capacity retention at 15 mAh over 1,400 cycles. To further reduce the cost of Mn-H batteries, the development of highly active and earth-abundant HER/HOR electrocatalysts is necessary. A thorough understanding of the release and handling of gaseous hydrogen is still required. The recent aqueous batteries based on the Mn deposition/dissolution chemistry with diverse anodes are listed in (Table 2).

7 Conclusion and outlook

Rechargeable aqueous Mn batteries are promising systems for storing energy sustainably owing to their safety, reasonably high voltage, and low-cost. Initially, the use of mild acidic electrolytes allowed aqueous Mn batteries to be rechargeable. Since then, our understanding of the working mechanism of rechargeable aqueous Mn batteries has progressed significantly. Rational electrolyte design enables the utilization of the high-potential MnO_2/Mn^{2+} redox couple, allowing for high-energy storage. The use of electrolyte additives can promote facile reaction kinetics and stable cycling performance. To obtain robust performances of rechargeable aqueous Mn batteries based on MnO_2/Mn^{2+} redox, suitable redox couples on the anode have been sought.

This includes metal dissolution/deposition (Sn, Cu, Bi, and Al), $Pb/PbSO_4$ redox, Na^+ adsorption/desorption, and hydrogen evolution/reduction reaction. Thus, overall, the underlying reaction mechanism in the aqueous batteries involving MnO_2/Mn^{2+} redox couple associated with the different anode environments is schematically illustrated in Figure 6.

8 Roadblocks need to be overcome

1. In view of the complexity of the redox reaction that takes place in both the deposition and dissolution voltage ranges of the aqueous batteries, the electrochemical stability window must be analyzed, and its true potential can only be realized at high arial mass loadings. Since the battery is charged or discharged with a high probability of accumulation of by-products, there is a serious challenge with the reversibility of charge or discharge capacity and the volume expansion associated with battery failure problems.
2. In most studies, the active materials are dissolved in the electrolyte rather than loaded into the electrode. Therefore, the stability of the electrolyte must be considered with the utmost care. This would have a excellent impact on battery performance in different operating environments.
3. Although various metal anodes are being tested for the aqueous batteries with the MnO_2/Mn^{2+}redox couple, the most significant and unavoidable challenge may be anode protection. The high reactivity of metal anodes in aqueous electrolytes and their dendritic challenges for battery failure are not yet considered in detail, which is a vital future research activity.

Author contributions

VS: Writing–original draft, Writing–review and editing. SN: Formal Analysis, Investigation, Supervision, Validation, Writing–review and editing. AM: Formal Analysis, Supervision, Writing–review and editing. GS: Investigation, Supervision, Writing–review and editing. AA: Formal Analysis, Supervision, Validation, Visualization, Writing–review and editing. DT: Funding acquisition, Project administration, Supervision, Writing–review and editing. JuK: Formal Analysis, Project administration, Supervision, Validation, Visualization, Writing–review and editing. Jak: Funding acquisition, Resources, Supervision, Writing–review and editing.

Funding

The author(s) declare financial support was received for the research, authorship, and/or publication of this article. This work was supported by the National Research Foundation of Korea (NRF) grant funded by the Korean government (MSIT) (NRF-2020R1A2C3012415 and NRF-2018R1A5A1025224). This research is also funded by Hanoi University of Science and Technology (HUST) under project number T2022-XS-001.

Acknowledgments

AA thank the Ministry for Culture and Science of North Rhine Westphalia (Germany) for funding within the International Graduate School for Battery Chemistry, Characterization, Analysis, Recycling and Application (BACCARA). The authors greatly acknowledge Andre Bar for his fantastic graphics support.

Conflict of interest

The authors declare that the research was conducted in the absence of any commercial or financial relationships that could be construed as a potential conflict of interest.

Publisher's note

References

Aguilar, I., Lemaire, P., Ayouni, N., Bendadesse, E., Morozov, A. V., Sel, O., et al. (2022). Identifying interfacial mechanisms limitations within aqueous Zn-MnO_2 batteries and means to cure them with additives. *Energy Storage Mater.* 53, 238–253. doi:10.1016/j.ensm.2022.08.043

Alfaruqi, M. H., Mathew, V., Gim, J., Kim, S., Song, J., Baboo, J. P., et al. (2015). Electrochemically induced structural transformation in a γ-MnO_2 cathode of a high capacity zinc-ion battery system. *Chem. Mat.* 27, 3609–3620. doi:10.1021/cm504717p

Ao, H., Zhao, Y., Zhou, J., Cai, W., Zhang, X., Zhu, Y., et al. (2019). Rechargeable aqueous hybrid ion batteries: developments and prospects. *J. Mater. Chem. A* 7, 18708–18734. doi:10.1039/C9TA06433H

Balland, V., Mateos, M., Singh, A., Harris, K. D., Laberty-Robert, C., and Limoges, B. (2021). The role of Al^{3+}-based aqueous electrolytes in the charge storage mechanism of MnO_x cathodes. *Small* 17, 2101515. doi:10.1002/smll.202101515

Chen, H., Cai, S., Wu, Y., Wang, W., Xu, M., and Bao, S.-J. (2021a). Successive electrochemical conversion reaction to understand the performance of aqueous Zn/MnO_2 batteries with Mn^{2+} additive. *Mater. Today Energy* 20, 100646. doi:10.1016/j.mtener.2021.100646

Chen, S., Sun, P., Humphreys, J., Zou, P., Zhang, M., Jeerh, G., et al. (2021). Acetate-based 'oversaturated gel electrolyte' enabling highly stable aqueous Zn-MnO_2 battery. *Energy Storage Mater.* 42, 240–251. doi:10.1016/j.ensm.2021.07.033

Chen, T., Zhang, X.-P., Wang, J., Li, J., Wu, C., Hu, M., et al. (2020). A review on electric vehicle charging infrastructure development in the UK. *J. Mod. Power Syst. Clean Energy* 8, 193–205. doi:10.35833/MPCE.2018.000374

Chen, W., Li, G., Pei, A., Li, Y., Liao, L., Wang, H., et al. (2018). A manganese–hydrogen battery with potential for grid-scale energy storage. *Nat. Energy* 3, 428–435. doi:10.1038/s41560-018-0147-7

Chuai, M., Yang, J., Wang, M., Yuan, Y., Liu, Z., Xu, Y., et al. (2021). High-performance Zn battery with transition metal ions co-regulated electrolytic MnO_2. *eScience* 1, 178–185. doi:10.1016/j.esci.2021.11.002

Dai, L., Wang, Y., Sun, L., Ding, Y., Yao, Y., Yao, L., et al. (2021). Jahn–teller distortion induced Mn^{2+}-rich cathode enables optimal flexible aqueous high-voltage Zn-Mn batteries. *Adv. Sci.* 8, 2004995. doi:10.1002/advs.202004995

Deng, Y., Wang, H., Fan, M., Zhan, B., Zuo, L.-J., Chen, C., et al. (2023). Nanomicellar electrolyte to control release ions and reconstruct hydrogen bonding network for ultrastable high-energy-density Zn–Mn battery. *J. Am. Chem. Soc.* 145, 20109–20120. doi:10.1021/jacs.3c07764

Durena, R., and Zukuls, A. (2023). A short review: comparison of zinc-manganese dioxide batteries with different pH aqueous electrolytes. *Batteries* 9, 311. doi:10.3390/batteries9060311

Feng, K., Wang, D., and Yu, Y. (2023). Progress and prospect of Zn anode modification in aqueous zinc-ion batteries: experimental and theoretical aspects. *Molecules* 28, 2721. doi:10.3390/molecules28062721

Feng, Y., Zhang, Q., Liu, S., Liu, J., Tao, Z., and Chen, J. (2019). A novel aqueous sodium–manganese battery system for energy storage. *J. Mater. Chem. A* 7, 8122–8128. doi:10.1039/C9TA00474B

Guo, X., Zhou, J., Bai, C., Li, X., Fang, G., and Liang, S. (2020). Zn/MnO_2 battery chemistry with dissolution-deposition mechanism. *Mater. Today Energy* 16, 100396. doi:10.1016/j.mtener.2020.100396

He, S., Wang, J., Zhang, X., Chen, J., Wang, Z., Yang, T., et al. (2019). A high-energy aqueous aluminum-manganese battery. *Adv. Funct. Mater.* 29, 1905228. doi:10.1002/adfm.201905228

Huang, J., Chi, X., Wu, J., Liu, J., and Liu, Y. (2022). High-concentration dual-complex electrolyte enabled a neutral aqueous zinc-manganese electrolytic battery with superior stability. *Chem. Eng. J.* 430, 133058. doi:10.1016/j.cej.2021.133058

Huang, J., Guo, Z., Dong, X., Bin, D., Wang, Y., and Xia, Y. (2019a). Low-cost and high safe manganese-based aqueous battery for grid energy storage and conversion. *Sci. Bull.* 64, 1780–1787. doi:10.1016/j.scib.2019.09.020

Huang, J., Tang, X., Liu, K., Fang, G., He, Z., and Li, Z. (2020a). Interfacial chemical binding and improved kinetics assisting stable aqueous Zn–MnO_2 batteries. *Mater. Today Energy* 17, 100475. doi:10.1016/j.mtener.2020.100475

Huang, J., Xie, Y., Yan, L., Wang, B., Kong, T., Dong, X., et al. (2021). Decoupled amphoteric water electrolysis and its integration with Mn–Zn battery for flexible utilization of renewables. *Energy Environ. Sci.* 14, 883–889. doi:10.1039/D0EE03639K

Huang, J., Yan, L., Bin, D., Dong, X., Wang, Y., and Xia, Y. (2020b). An aqueous manganese–lead battery for large-scale energy storage. *J. Mater. Chem. A* 8, 5959–5967. doi:10.1039/D0TA01484B

Huang, Y., Mou, J., Liu, W., Wang, X., Dong, L., Kang, F., et al. (2019b). Novel insights into energy storage mechanism of aqueous rechargeable Zn/MnO_2 batteries with participation of Mn^{2+}. *Nanomicro Lett.* 11, 49. doi:10.1007/s40820-019-0278-9

Islam, S., Alfaruqi, M. H., Mathew, V., Song, J., Kim, S., Kim, S., et al. (2017). Facile synthesis and the exploration of the zinc storage mechanism of β-MnO_2 nanorods with exposed (101) planes as a novel cathode material for high performance eco-friendly zinc-ion batteries. *J. Mater. Chem. A* 5, 23299–23309. doi:10.1039/C7TA07170A

Islam, S., Alfaruqi, M. H., Putro, D. Y., Park, S., Kim, S., Lee, S., et al. (2021). *In situ* oriented Mn deficient $ZnMn_2O_4$@C nanoarchitecture for durable rechargeable aqueous zinc-ion batteries. *Adv. Sci.* 8, 2002636. doi:10.1002/advs.202002636

Kankanallu, V. R., Zheng, X., Leschev, D., Zmich, N., Clark, C., Lin, C.-H., et al. (2023). Elucidating a dissolution–deposition reaction mechanism by multimodal synchrotron X-ray characterization in aqueous Zn/MnO_2 batteries. *Energy Environ. Sci.* 16, 2464–2482. doi:10.1039/D2EE03731A

Kim, B., Kim, Y. S., Dulyawat, D., and Chung, C.-H. (2023). Development of a Zn-Mn aqueous redox-flow battery operable at 2.4 V of discharging potential in a hybrid cell with an Ag-decorated carbon-felt electrode. *J. Energy Storage* 72, 108337. doi:10.1016/j.est.2023.108337

Kim, S. H., and Oh, S. M. (1998). Degradation mechanism of layered MnO_2 cathodes in Zn/$ZnSO_4$/MnO_2 rechargeable cells. *J. Power Sources* 72, 150–158. doi:10.1016/S0378-7753(97)02703-1

Kordesch, K., Gsellmann, J., Peri, M., Tomantschger, K., and Chemelli, R. (1981). The rechargeability of manganese dioxide in alkaline electrolyte. *Electrochimica Acta* 26, 1495–1504. doi:10.1016/0013-4686(81)90021-9

Kurzweil, P. (2010). Gaston Planté and his invention of the lead–acid battery—the genesis of the first practical rechargeable battery. *J. Power Sources* 195, 4424–4434. doi:10.1016/j.jpowsour.2009.12.126

Larcher, D., and Tarascon, J. M. (2015). Towards greener and more sustainable batteries for electrical energy storage. *Nat. Chem.* 7, 19–29. doi:10.1038/nchem.2085

Lee, B., Seo, H. R., Lee, H. R., Yoon, C. S., Kim, J. H., Chung, K. Y., et al. (2016). Critical role of pH evolution of electrolyte in the reaction mechanism for rechargeable zinc batteries. *ChemSusChem* 9, 2948–2956. doi:10.1002/cssc.201600702

Lee, J., Ju, J. B., Cho, W.Il, Cho, B. W., and Oh, S. H. (2013). Todorokite-type MnO_2 as a zinc-ion intercalating material. *Electrochimica Acta* 112, 138–143. doi:10.1016/j.electacta.2013.08.136

Lei, J., Yao, Y., Huang, Y., and Lu, Y.-C. (2023). A highly reversible low-cost aqueous sulfur–manganese redox flow battery. *ACS Energy Lett.* 8, 429–435. doi:10.1021/acsenergylett.2c02524

Lei, J., Yao, Y., Wang, Z., and Lu, Y.-C. (2021). Towards high-areal-capacity aqueous zinc–manganese batteries: promoting MnO_2 dissolution by redox mediators. *Energy Environ. Sci.* 14, 4418–4426. doi:10.1039/D1EE01120K

Li, W., Dahn, J. R., and Wainwright, D. S. (1994). Rechargeable lithium batteries with aqueous electrolytes. *Science* 264, 1115–1118. doi:10.1126/science.264.5162.1115

Li, X., Tang, Y., Han, C., Wei, Z., Fan, H., Lv, H., et al. (2023). A static tin–manganese battery with 30000-cycle lifespan based on stabilized Mn^{3+}/Mn^{2+} redox chemistry. *ACS Nano* 17, 5083–5094. doi:10.1021/acsnano.3c00242

Li, Y., Wang, S., Salvador, J. R., Wu, J., Liu, B., Yang, W., et al. (2019). Reaction mechanisms for long-life rechargeable Zn/MnO_2 batteries. *Chem. Mater.* 31, 2036–2047. doi:10.1021/acs.chemmater.8b05093

Liang, G., Mo, F., Li, H., Tang, Z., Liu, Z., Wang, D., et al. (2019). A universal principle to design reversible aqueous batteries based on deposition–dissolution mechanism. *Adv. Energy Mater.* 9, 1901838. doi:10.1002/aenm.201901838

Liang, R., Fu, J., Deng, Y.-P., Pei, Y., Zhang, M., Yu, A., et al. (2021). Parasitic electrodeposition in Zn-MnO_2 batteries and its suppression for prolonged cyclability. *Energy Storage Mater.* 36, 478–484. doi:10.1016/j.ensm.2020.12.015

Lim, M. B., Lambert, T. N., and Chalamala, B. R. (2021). Rechargeable alkaline zinc–manganese oxide batteries for grid storage: mechanisms, challenges and developments. *Mater. Sci. Eng. R Rep.* 143, 100593. doi:10.1016/j.mser.2020.100593

Liu, J., Xu, C., Chen, Z., Ni, S., and Shen, Z. X. (2018). Progress in aqueous rechargeable batteries. *Green Energy & Environ.* 3, 20–41. doi:10.1016/j.gee.2017.10.001

Liu, Y., Lin, J., Miao, X., Chen, Y., Zhang, X., Chen, S., et al. (2020a). A simple aqueous battery with potential for scalable energy storage based on MnO_2 deposition at the cathode and a quinoid-modified activated carbon anode. *ChemElectroChem* 7, 2869–2876. doi:10.1002/celc.202000481

Liu, Y., Qin, Z., Yang, X., Liu, J., Liu, X.-X., and Sun, X. (2023). Voltage induced lattice contraction enabling superior cycling stability of MnO_2 cathode in aqueous zinc batteries. *Energy Storage Mater.* 56, 524–531. doi:10.1016/j.ensm.2023.01.041

Liu, Y., Zhi, J., Sedighi, M., Han, M., Shi, Q., Wu, Y., et al. (2020b). Mn^{2+} ions confined by electrode microskin for aqueous battery beyond intercalation capacity. *Adv. Energy Mater.* 10, 2002578. doi:10.1002/aenm.202002578

Liu, Z., Qin, L., Chen, X., Xie, X., Zhu, B., Gao, Y., et al. (2021a). Improving stability and reversibility via fluorine doping in aqueous zinc–manganese batteries. *Mater. Today Energy* 22, 100851. doi:10.1016/j.mtener.2021.100851

Liu, Z., Qin, L., Lu, B., Wu, X., Liang, S., and Zhou, J. (2022a). Issues and opportunities facing aqueous $Mn^{(2+)}$/MnO_2-based batteries. *ChemSusChem* 15, 202200348. doi:10.1002/cssc.202200348

Liu, Z., Yang, Y., Liang, S., Lu, B., and Zhou, J. (2021b). pH-buffer contained electrolyte for self-adjusted cathode-free Zn–MnO_2 batteries with coexistence of dual mechanisms. *Small Struct.* 2, 2100119. doi:10.1002/sstr.202100119

Liu, Z., Yang, Y., Lu, B., Liang, S., Fan, H. J., and Zhou, J. (2022b). Insights into complexing effects in acetate-based Zn-MnO_2 batteries and performance enhancement by all-round strategies. *Energy Storage Mater.* 52, 104–110. doi:10.1016/j.ensm.2022.07.043

Lv, H., Song, Y., Qin, Z., Zhang, M., Yang, D., Pan, Q., et al. (2022). Disproportionation enabling reversible MnO_2/Mn^{2+} transformation in a mild aqueous Zn-MnO_2 hybrid battery. *Chem. Eng. J.* 430, 133064. doi:10.1016/j.cej.2021.133064

Mateos, M., Makivic, N., Kim, Y.-S., Limoges, B., and Balland, V. (2020). Accessing the two-electron charge storage capacity of MnO_2 in mild aqueous electrolytes. *Adv. Energy Mater.* 10, 2000332. doi:10.1002/aenm.202000332

Mathew, V., Sambandam, B., Kim, S., Kim, S., Park, S., Lee, S., et al. (2020). Manganese and vanadium oxide cathodes for aqueous rechargeable zinc-ion batteries: a focused view on performance, mechanism, and developments. *ACS Energy Lett.* 5, 2376–2400. doi:10.1021/acsenergylett.0c00740

Ming, J., Guo, J., Xia, C., Wang, W., and Alshareef, H. N. (2019). Zinc-ion batteries: materials, mechanisms, and applications. *Mater. Sci. Eng. R Rep.* 135, 58–84. doi:10.1016/j.mser.2018.10.002

Moon, H., Ha, K.-H., Park, Y., Lee, J., Kwon, M.-S., Lim, J., et al. (2021). Direct proof of the reversible dissolution/deposition of Mn^{2+}/Mn^{4+} for mild-acid Zn-MnO_2 batteries with porous carbon interlayers. *Adv. Sci.* 8, 2003714. doi:10.1002/advs.202003714

Naresh, R., Pol, V. G., and Ragupathy, P. (2023). Energy storage mechanism, advancement, challenges, and perspectives on vivid manganese redox couples. *Energy Adv.* 2, 948–964. doi:10.1039/D3YA00102D

Naresh, R. P., Mariyappan, K., Dixon, D., Ulaganathan, M., and Ragupathy, P. (2021). Investigations on new electrolyte composition and modified membrane for high voltage Zinc–Manganese hybrid redox flow batteries. *Batter. Supercaps* 4, 1464–1472. doi:10.1002/batt.202100071

Oka, K., Löfgren, R., Emanuelsson, R., Nishide, H., Oyaizu, K., Strømme, M., et al. (2020). Conducting redox polymer as organic anode material for polymer-manganese secondary batteries. *ChemElectroChem* 7, 3336–3340. doi:10.1002/celc.202000711

Pan, H., Shao, Y., Yan, P., Cheng, Y., Han, K. S., Nie, Z., et al. (2016). Reversible aqueous zinc/manganese oxide energy storage from conversion reactions. *Nat. Energy* 1, 16039. doi:10.1038/nenergy.2016.39

Perret, P. G., Malenfant, P. R., Bock, C., and MacDougall, B. (2011). A graphene "MnO_2" hybrid supercapacitor based on *in situ* electo-deposition and dissolution of "MnO_2". *ECS Trans.* 35, 195–205. doi:10.1149/1.3654218

Perret, P. G., Malenfant, P. R. L., Bock, C., and MacDougall, B. (2012). Electro-deposition and dissolution of MnO_2 on a graphene composite electrode for its utilization in an aqueous based hybrid supercapacitor. *J. Electrochem Soc.* 159, A1554–A1561. doi:10.1149/2.064208jes

Ruan, P., Chen, X., Qin, L., Tang, Y., Lu, B., Zeng, Z., et al. (2023). Achieving highly proton-resistant Zn–Pb anode through low hydrogen affinity and strong bonding for long-life electrolytic Zn//MnO_2 battery. *Adv. Mater.* 35, 2300577. doi:10.1002/adma.202300577

Sambandam, B., Mathew, V., Kim, S., Lee, S., Kim, S., Hwang, J. Y., et al. (2022). An analysis of the electrochemical mechanism of manganese oxides in aqueous zinc batteries. *Chem* 8, 924–946. doi:10.1016/j.chempr.2022.03.019

Sambandam, B., Soundharrajan, V., Kim, S., Alfaruqi, M. H., Jo, J., Kim, S., et al. (2018a). Aqueous rechargeable Zn-ion batteries: an imperishable and high-energy $Zn_2V_2O_7$ nanowire cathode through intercalation regulation. *J. Mater. Chem. A* 6, 3850–3856. doi:10.1039/C7TA11237H

Sambandam, B., Soundharrajan, V., Kim, S., Alfaruqi, M. H., Jo, J., Kim, S., et al. (2018b). $K_2V_6O_{16}{\cdot}2.7H_2O$ nanorod cathode: an advanced intercalation system for high energy aqueous rechargeable Zn-ion batteries. *J. Mater. Chem. A* 6, 15530–15539. doi:10.1039/C8TA02018C

Scarfogliero, M., Carmeli, S., Castelli-Dezza, F., Mauri, M., Rossi, M., Marchegiani, G., et al. (2018). "Lithium-ion batteries for electric vehicles: a review on aging models for vehicle-to-grid services," in 2018 International Conference of Electrical and Electronic Technologies for Automotive, 1–6. doi:10.23919/EETA.2018.8493211

Shen, X., Wang, X., Zhou, Y., Shi, Y., Zhao, L., Jin, H., et al. (2021a). Highly reversible aqueous Zn-MnO_2 battery by supplementing Mn^{2+}-mediated MnO_2 deposition and dissolution. *Adv. Funct. Mater.* 31, 2101579. doi:10.1002/adfm.202101579

Shen, Z., Tang, Z., Li, C., Luo, L., Pu, J., Wen, Z., et al. (2021b). Precise proton redistribution for two-electron redox in aqueous zinc/manganese dioxide batteries. *Adv. Energy Mater.* 11, 2102055. doi:10.1002/aenm.202102055

Shin, J., and Choi, J. W. (2020). Opportunities and reality of aqueous rechargeable batteries. *Adv. Energy Mater.* 10, 2001386. doi:10.1002/aenm.202001386

Soundharrajan, V., Lee, J., Kim, S., Putro, D. Y., Lee, S., Sambandam, B., et al. (2022a). Aqueous rechargeable Zn/ZnO battery based on deposition/dissolution chemistry. *Molecules* 27, 8664. doi:10.3390/molecules27248664

Soundharrajan, V., Nithiananth, S., Lee, J., Kim, J. H. J., Hwang, J.-Y., Kim, J. H. J., et al. (2022b). LiV_3O_8 as an intercalation-type cathode for aqueous aluminum-ion batteries. *J. Mater. Chem. A* 10, 18162–18169. doi:10.1039/D2TA04823J

Soundharrajan, V., Nithiananth, S., Lee, J., Sakthiabirami, K., Pham, D. T., Kim, J. H., et al. (2023). Manganese ion batteries: LiV_3O_8 nanorods as a robust and long-life cathode module. *J. Power Sources* 558, 232542. doi:10.1016/j.jpowsour.2022.232542

Soundharrajan, V., Nithiananth, S., Sakthiabirami, K., Kim, J. H., Su, C.-Y., and Chang, J.-K. (2022c). The advent of manganese-substituted sodium vanadium

phosphate-based cathodes for sodium-ion batteries and their current progress: a focused review. *J. Mater. Chem. A* 10, 1022–1046. doi:10.1039/D1TA09040B

Soundharrajan, V., Sambandam, B., Kim, S., Islam, S., Jo, J., Kim, S., et al. (2020). The dominant role of Mn^{2+} additive on the electrochemical reaction in $ZnMn_2O_4$ cathode for aqueous zinc-ion batteries. *Energy Storage Mater.* 28, 407–417. doi:10.1016/j.ensm.2019.12.021

Soundharrajan, V., Sambandam, B., Kim, S., Mathew, V., Jo, J., Kim, S., et al. (2018). Aqueous magnesium zinc hybrid battery: an advanced high-voltage and high-energy $MgMn_2O_4$ cathode. *ACS Energy Lett.* 3, 1998–2004. doi:10.1021/acsenergylett.8b01105

Sun, J., Liu, Z., Li, K., Yuan, Y., Zheng, X., Xu, Y., et al. (2022). Proton-trapping agent for mitigating hydrogen evolution corrosion of Zn for an electrolytic MnO_2/Zn battery. *ACS Appl. Mater Interfaces* 14, 51900–51909. doi:10.1021/acsami.2c14370

Sun, W., Wang, F., Hou, S., Yang, C., Fan, X., Ma, Z., et al. (2017). Zn/MnO_2 battery chemistry with H^+ and Zn^{2+} coinsertion. *J. Am. Chem. Soc.* 139, 9775–9778. doi:10.1021/jacs.7b04471

Wang, M., Chen, N., Zhu, Z., Meng, Y., Shen, C., Zheng, X., et al. (2021). Electrodeless MnO_2-metal batteries with deposition and stripping chemistry. *Small* 17, 2103921. doi:10.1002/smll.202103921

Wei, L., Jiang, H. R., Ren, Y. X., Wu, M. C., Xu, J. B., and Zhao, T. S. (2019a). Investigation of an aqueous rechargeable battery consisting of manganese tin redox chemistries for energy storage. *J. Power Sources* 437, 226918. doi:10.1016/j.jpowsour.2019.226918

Wei, L., Zeng, L., Wu, M. C., Jiang, H. R., and Zhao, T. S. (2019b). An aqueous manganese-copper battery for large-scale energy storage applications. *J. Power Sources* 423, 203–210. doi:10.1016/j.jpowsour.2019.03.085

Wu, J., Yang, J., Leong, Z. Y., Zhang, F., Deng, H., Ouyang, G. F., et al. (2022). A method to inhibit disproportionation of Mn^{3+} for low-cost Mn–Fe all-flow battery. *ACS Appl. Energy Mater* 5, 14646–14651. doi:10.1021/acsaem.2c03075

Wu, T.-H., Lin, Y.-Q., Althouse, Z. D., and Liu, N. (2021). Dissolution–redeposition mechanism of the MnO_2 cathode in aqueous zinc-ion batteries. *ACS Appl. Energy Mater* 4, 12267–12274. doi:10.1021/acsaem.1c02064

Xie, C., Li, Y., Wang, Q., Sun, D., Tang, Y., and Wang, H. (2020). Issues and solutions toward zinc anode in aqueous zinc-ion batteries: a mini review. *Carbon Energy* 2, 540–560. doi:10.1002/cey2.67

Xu, C., Li, B., Du, H., and Kang, F. (2012). Energetic zinc ion chemistry: the rechargeable zinc ion battery. *Angew. Chem. Int. Ed.* 51, 933–935. doi:10.1002/anie.201106307

Xu, Q., Xie, Q.-X., Xue, T., Cheng, G., Wu, J.-D., Ning, L., et al. (2023). Salt Bridge-intermediated three phase decoupling electrolytes for high voltage electrolytic aqueous Zinc-Manganese dioxides battery. *Chem. Eng. J.* 451, 138775. doi:10.1016/j.cej.2022.138775

Xu, Y., Ma, J., Jiang, T., Ding, H., Wang, W., Wang, M., et al. (2022). Tuning electrolyte solvation structures to enable stable aqueous Al/MnO_2 battery. *Energy Storage Mater.* 47, 113–121. doi:10.1016/j.ensm.2022.01.060

Yamamoto, T., and Shoji, T. (1986). Rechargeable Zn|$ZnSO_4$|MnO_2-type cells. *Inorganica Chim. Acta* 117, L27–L28. doi:10.1016/S0020-1693(00)82175-1

Yang, H., Zhang, T., Chen, D., Tan, Y., Zhou, W., Li, L., et al. (2023). Protocol in evaluating capacity of Zn–Mn aqueous batteries: a clue of pH. *Adv. Mater.* 35, 2300053. doi:10.1002/adma.202300053

Yang, M., Chen, R., Shen, Y., Zhao, X., and Shen, X. (2020). A high-energy aqueous manganese–metal hydride hybrid battery. *Adv. Mater.* 32, 2001106. doi:10.1002/adma.202001106

Yang, X., Jia, Z., Wu, W., Shi, H.-Y., Lin, Z., Li, C., et al. (2022). The back-deposition of dissolved Mn^{2+} to MnO_2 cathodes for stable cycling in aqueous zinc batteries. *Chem. Commun.* 58, 4845–4848. doi:10.1039/D2CC00334A

Ye, X., Han, D., Jiang, G., Cui, C., Guo, Y., Wang, Y., et al. (2023). Unraveling the deposition/dissolution chemistry of MnO_2 for high-energy aqueous batteries. *Energy Environ. Sci.* 16, 1016–1023. doi:10.1039/D3EE00018D

Yu, Y., Xie, J., Zhou, L., Yang, F., Zhang, H., Liu, X., et al. (2022). A high-voltage aqueous antimony-manganese hybrid battery based on all stripping/plating mechanism. *Energy Storage Mater.* 49, 529–536. doi:10.1016/j.ensm.2022.04.037

Yu, Y., Zhang, H., Yang, F., Zeng, Y., Liu, X., and Lu, X. (2021). Bismuth nanoparticles@carbon composite as a stable and high capacity anode for high-voltage bismuth-manganese batteries. *Energy Storage Mater.* 41, 623–630. doi:10.1016/j.ensm.2021.06.042

Yuan, C., Zhang, Y., Pan, Y., Liu, X., Wang, G., and Cao, D. (2014). Investigation of the intercalation of polyvalent cations (Mg^{2+}, Zn^{2+}) into λ-MnO_2 for rechargeable aqueous battery. *Electrochimica Acta* 116, 404–412. doi:10.1016/j.electacta.2013.11.090

Zeng, X., Hao, J., Wang, Z., Mao, J., and Guo, Z. (2019). Recent progress and perspectives on aqueous Zn-based rechargeable batteries with mild aqueous electrolytes. *Energy Storage Mater.* 20, 410–437. doi:10.1016/j.ensm.2019.04.022

Zhang, M., Wu, W., Luo, J., Zhang, H., Liu, J., Liu, X., et al. (2020a). A high-energy-density aqueous zinc–manganese battery with a La–Ca co-doped ε-MnO_2 cathode. *J. Mater. Chem. A* 8, 11642–11648. doi:10.1039/D0TA03706K

Zhang, T., Zhang, S., Cao, S., Yao, Q., and Lee, J. Y. (2020b). Bridging the energy efficiency gap between quasi-neutral and alkaline rechargeable zinc-air batteries by an efficient hybrid battery design. *Energy Storage Mater.* 33, 181–187. doi:10.1016/j.ensm.2020.08.019

Zhao, S., Han, B., Zhang, D., Huang, Q., Xiao, L., Chen, L., et al. (2018). Unravelling the reaction chemistry and degradation mechanism in aqueous Zn/MnO_2 rechargeable batteries. *J. Mater. Chem. A* 6, 5733–5739. doi:10.1039/C8TA01031E

Zheng, X., Wang, Y., Xu, Y., Ahmad, T., Yuan, Y., Sun, J., et al. (2021). Boosting electrolytic MnO_2–Zn batteries by a bromine mediator. *Nano Lett.* 21, 8863–8871. doi:10.1021/acs.nanolett.1c03319

Zhong, C., Liu, B., Ding, J., Liu, X., Zhong, Y., Li, Y., et al. (2020). Decoupling electrolytes towards stable and high-energy rechargeable aqueous zinc–manganese dioxide batteries. *Nat. Energy* 5, 440–449. doi:10.1038/s41560-020-0584-y

Zhong, Z., Li, J., Li, L., Xi, X., Luo, Z., Fang, G., et al. (2022). Improving performance of zinc-manganese battery via efficient deposition/dissolution chemistry. *Energy Storage Mater.* 46, 165–174. doi:10.1016/j.ensm.2022.01.006

Zhu, Z., Jiang, T., Ali, M., Meng, Y., Jin, Y., Cui, Y., et al. (2022). Rechargeable batteries for grid scale energy storage. *Chem. Rev.* 122, 16610–16751. doi:10.1021/acs.chemrev.2c00289